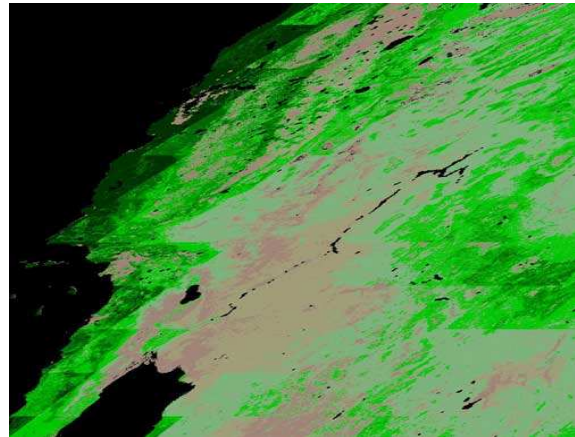Centre for Geo-Information

Thesis Report GIRS-2008-06

ESTIMATING NPP BY INTEGRATING REAL-TIME SENSOR DATA AND REMOTE SENSING DATA

BEATUS JACOB CHUMA

MARCH 2008

WAGENINGEN UNIVERSITY
WAGENINGEN UR

II

ESTIMATING NPP BY INTEGRATING REAL-TIME SENSOR DATA AND REMOTE SENSING DATA

BEATUS JACOB CHUMA

Registration number 71 11 11 157 120

<u>Supervisors</u>:

Dr. Bruin Sytze de
Dr. Kooistra Lammert

A thesis submitted in partial fulfilment of the degree of Master of Science
at Wageningen University and Research Centre,
The Netherlands.

March 2006
Wageningen, The Netherlands

Foreword

This report represents six months of research on estimating NPP by integrating real-time sensor data and remote sensing data. The report is my MSc. thesis done as part of the Master of Science in Geo-Information Science (MGI) at the Wageningen University.

My deep appreciation goes to my supervisors Dr. Bruin Sytze de and Dr. Kooistra Lammert for their invaluable encouragements, ideas, suggestions and patience during my research work. Without their advice and support this thesis would never become feasible. I wish that the demonstrated method in this thesis is the first step to assess its applicability and efficiency at local scale level.

I would like to extend my special thanks to my wife Victoria and son Beatus for their courage and support during the entire period of my thesis work. Lastly, I am grateful to all MGI students whose moral, spiritual, psycho-emotional and material support assisted in making this work successful.

Beatus Jacob Chuma, March 2008

TABLE OF CONTENTS

LIST OF FIGURES

ABBREVIATIONS

APAR	Absorbed Photosynthetically Active Radiation
AVHRR	Advanced Very High Resolution Radiometer
CASA	Carnegie-Ames-Stanford-Approach
EOS	Earth Observing System
EO	Earth Observation
fPAR	Fraction of Photosynthetically Active Radiation
GLO-PEM	Global Production Efficiency Model
GPP	Gross Primary Production (g C m^{-2} day $^{-1}$)
LAI	Leaf Area Index
LUE	Light Use Efficiency
MODIS	Moderate-resolution Imaging Spectroradiometer
MOD17A2	MODIS/Terra Gross Primary Productivity 8-Day L3 Global 1km SIN Grid V005
MOD17A3	MODIS/Terra Net Primary Production Yearly L4 Global 1km SIN Grid
MOD09GQ	MODIS/Terra Surface Reflectance Daily L2G Global 250m SIN Grid
MRT	MODIS reprojection tool
NDVI	Normalised Difference Vegetation Index
NIR	Near-Infra Red
nm	Nanometer
NPP	Net Primary Production [gCm^{-2}year^{-1}]
PAR	Photosynthetically Active Radiation
PEMs	Production efficiency models
PRI	Photochemical Reflectance Index
SDBM	Simple Diagnostic Biosphere Model
SWE	Sensor web Enablement
SWRad	Shortwave radiation
TURC	Terrestrial Uptake and Release of Carbon
VPD	Vapour Pressure Deficit

ABSTRACT

The light use efficiency (LUE) approach is often used with remotely sensed data products and meteorological data to estimate net primary production (NPP) from local to global scales. To estimate local NPP, detailed information of spatial and temporal dynamic change on vegetation within local landscape is increasingly important. Recently, the advancement of technology in sensor web has shown to be promising for improving the estimation of local NPP due to its ability to provide real-time data. Still the challenge ahead to researchers is how to integrate remote sensing and the sensor web data with variability in spatial and temporal scale for better estimation of NPP at local level. The objective of this study was to demonstrate a method for acquiring local NPP estimations by integrating remote sensing and sensor web data at Gendt location.

The light use efficiency model has been found to be more appropriate for NPP estimation at local scale level in comparison to other methods and was adopted in this thesis. Spatial variability in remote sensing datasets were harmonized into common resolution based on aggregation technique while temporal variability in sensor web datasets were harmonized into daily time step based on integration and average techniques. Therefore, LUE method was used to integrate the remote sensing and sensor web data and the results were investigated by comparing them with two coarse scale MODIS standard products. The results attained from LUE model shows that high annual NPP values were obtained for cropland and grassland compared to other vegetation types. The comparison was done based on the derived daily GPP and annual NPP 2007 with MODIS product 8 days GPP (MOD17A2) and annual NPP (MOD17A3) 2006. Correlations were found at some locations with cropland and grassland for GPP while no correlation was found for annual NPP, though at some locations with grassland and cropland the values of NPP seemed to be much closer. Sources for the difference in results were identified as change in management of the parcel/size or land use types at some locations within the study area since the comparison was based on different years. The use of different light use efficiencies in the estimation of daily GPP is also considered as a source of differences. Additionally, the use of different parameters in the estimation of growth and maintenance respiration were recognized as sources. The demonstrated method was successful for data integration but the validity of the results obtained need further study.

Keywords: Gross primary production, Net primary production, Light use efficiency, MODIS, Remote sensing, In-situ sensing (sensor web).

1 INTRODUCTION

1.1 Background

Net primary production (NPP) is the net amount of solar energy converted to plant organic matter through photosynthesis. It is the rate at which vegetation in an ecosystem fixes CO_2 from the atmosphere (gross primary productivity, GPP) minus the rate at which the vegetation returns CO_2 to the atmosphere through plant respiration. In recent years, modeling NPP of terrestrial ecosystems has been a subject of increasing interest because of concerns about the global terrestrial carbon cycle in relation to climate change.

The practical importance of NPP is in its utility as a measure of crop yield, forest production (Milner et al., 1996), and other economically and socially significant product of vegetation growth. Regular monitoring of global terrestrial net primary production (NPP) and gross primary production (GPP) is needed for the purposes of evaluating trends in biospheric behavior (Nemani et al., 2003), and investigating large-scale patterns in food and fiber production(Running et al., 2004). Consequently, estimating global primary productivity and monitoring changes will play an important role in detecting the state of biosphere.

At the global scale, terrestrial NPP is one of the most-modeled ecological parameters, with models that differ markedly in approach and complexity often yielding comparable estimates (Field et al., 1995). Field et al. (1995) also noted that similarities at global scale reveal little about a model's ability to estimate local or regional NPP, NPP for subannual time increments, or NPP under conditions of changed climate or species distributions (Field et al., 1995).

At the local scale, NPP can be defined and measured in two experimental ways as biomass produced during the growing season or as net gas exchange of plants, namely, the difference between gross primary production (GPP) and autotrophic respiration (Churkina and Running, 1998). However, measurements based on biomass data are by far the most common. Measurements based on biomass must confront the challenge of quantifying below ground processes, including root production and exudation (Sala et al., 1988). Measurements based on gas exchange are complicated by the fact that it is very difficult to measure either GPP or autotrophic respiration (Ra) in isolation. Gas exchange measurements at the leaf scale typically measure the sum of photosynthesis and leaf respiration.

Satellite remote sensing is an attractive tool for crop area and NPP estimates because it provides spatial and temporal information on the location and state of crop canopies. Recent advances in remote sensing, in terms of both new sensors and algorithm development for data processing, have shown a promising potential for doing near real-time monitoring of key biophysical parameters of vegetation, for input into an ecosystem model. This includes consistent and timely availability of land surface products from EOS/MODIS.

In the last few years, a coordinated strategy has been developed to improve estimates of terrestrial net and gross primary productivity by integrating multiple, complementary and independent data sources. This is because environmental conditions change over the earth's surface, consequently, NPP of terrestrial vegetation varies over space and time. Spatial variations of NPP are related to factors such as climate, vegetation distribution, and land use across the planet from local to global scales (Cao et al., 2004). The advanced technologies of today make it possible to develop integrated approaches to Earth sensing that encompass both remote and in-situ sensing. The ongoing challenge to scientific researchers is how to develop the approach that integrates an in-situ sensor web and remote sensing imagery data to provide superior estimates and predictions of biomass, and crop yield.

Different approaches have been used to estimate carbon exchange from regional to global scales (Goetz and Prince, 1999). Ecosystem models play an important role in synthesizing such disparate time/space data into single coherent analysis of terrestrial carbon fluxes. However, the applicability of such models at an operational level is often limited by the fundamental drawback of large input parameter requirements, for which some may require acquisition in near real time (Hazarika et al., 2005).

The recent advancement of sensor web technology has shown a promising potential in the analysis of temporal dynamic change on vegetation conditions within local landscape. Information/measurement from sensor web is one of the key variables driving ecosystems at local to global scales. Sufficient availability of real-time sensor web data has increased the understanding and detection of vegetation status of varied landscape. This has increased the opportunity of better estimation local NPP where land use variability is dominant across landscape.

1.2 Problem definition

Net primary production is highly variable in space and time. Spatial variations of NPP are related to factors such as climate, vegetation distribution, and land use across the planet from local to global scales (Cao et al., 2004). In understanding the spatial variability of NPP at the local scale level, detailed information in particular vegetation distribution and climatology at large spatial scale is highly important. Therefore, NPP estimation at local scale level has much influence on detailed and finer resolution dataset both spatial and temporal.

Different literature sources have tried to documents several methods used to estimate NPP from regional to global. Some of these methods are used remote sensing data while others are combined remote sensing and meteorological data. However, application of these datasets can easily be distinguished based on local or global scaling. Detection of current status of vegetation growth or net primary productivity at local level can only be determined with detailed information on landscape variability and highly temporal resolution datasets. Such information is difficult to acquire based on one type of dataset either remote sensing or meteorological data. Though remote sensing is now days available in real time such as MODIS product but its coarse scale has been a drawback in use at local level. Their resolution ranges from 250m to 1km for the MODIS instruments and to 1km and above for the other instruments (Chien et al., 2005). In general remote sensing is still recognized for providing spatial detailed information at local level though in low temporal scaling. Recently, the advancement of sensor web technology has been recognized for providing real time data which is useful in temporal scientific application. Based on local NPP estimation, these sensor web data with high temporal scaling is more significant in detecting current vegetation condition. Therefore, local NPP can be better estimated by combining or integrating different data sources.

In the past, carbon budgets and estimates of NPP have mostly been calculated on a yearly basis. Recent technological developments in continuous measurements have made it possible to make NPP estimates with a daily time resolution. This is more profound in detecting temporal dynamic change of vegetation within local landscape. The advancement of today's technologies has made it possible to develop integrated approaches to Earth sensing that encompass both remote and in-situ sensing (Teillet et al., 2005). So far there is only limited number of published literatures on methods for combining real-time sensor web data and

remote sensing data for improving NPP estimation. Therefore it is the aim of this research to develop a method that will integrate sensor web and remote sensing for the purpose of better estimation of NPP productivity at local scale level. It is the intent of this research to apply the method at Gendt area as a test case and examine the possibility of implementing the same approach elsewhere. The derived NPP productivity will be compared with MODIS product (MOD17A2/A3). This is an important step for this research in order to understand and quantify the quality and accuracy of the results.

1.3   Research objectives

The aim of this thesis is to demonstrate a method for integrating remote sensing and sensor web for estimation of NPP at the Gendt area along the Waal (near the city of Nijmegen). This objective is achieved by:

- Assessing the potential of combining real-time sensor web data with earth observation data for mapping NPP (with the purpose of estimating crop productivity).
- Generating a time series of NPP maps for vegetation area.

1.4   Research questions

1. Which possibilities existing for integration of remote sensing data and sensor web data for NPP estimation?
2. Which method can be implemented for NPP estimation in the present study and how can this method be parameterized?
3. Which methods can be used to deal with differences in spatial and temporal resolution of different data sources?
4. Are the results consistent with MODIS products (MOD17A2 and MOD17A3)? In case of differences can these be explained?
5. Which are the possibilities for data comparison and Validation to assess the quality of the developed NPP estimation method?
6. Can the method approach of the research be applied elsewhere?

1.5   Report outline

The general background information of the research was introduced in chapter one. This includes the problem definition, research objectives, research questions, and report outline. Chapter two reviews methods for integration remote sensing data and sensor web data for NPP estimation. Model parameterization and data requirements are also discussed in this chapter. The implementation of the method used in this study is discussed in Chapter three. Preprocessing of meteorological data, the implementation of a local light use efficiency model for GPP/NPP estimation, and methods comparison are all documented in this chapter. Chapter four presents the results of the application of the method on the Gendt area. Also a comparison of the derived GPP/NPP with (standard) MODIS products is made. Chapter five discusses the results of the case study. Finally, chapter 6 lists the conclusions and recommendations raised from the study. In the conclusion, the results are discussed with regards to the research questions. The appendices given at the end of the report contained the scripts used in this thesis.

2 LITERATURE REVIEW

2.1 Overview - NPP model

For many years remote sensing techniques have been recognized for NPP estimation at regional to global scale levels. Recently, much attention has been given to the development of method(s) that can integrate different data sources to improve NPP estimation. Since then, different methods have been developed for NPP estimation and these methods differ in terms of on factors such as the resolution of the input data, global or regional scale, use of biophysical factors or climate variables parametric models, ways of processing, and general assumptions. The method used for NPP estimates can be discussed in three broad categories, namely; light-use efficiency (LUE) approach, climate dependent approach and other (land-biosphere) models. Light use efficiency approach uses remote sensing and meteorological data in the estimation of NPP. The climate dependent approach uses empirical relationships between climate variables and vegetation attributes such as cover types, allowing NPP to be estimated as a function of climate variables such as temperature, precipitation, and evapotranspiration. This thesis will explore and review the method that is capable of integrating remote sensing and sensor web.

2.2 NPP modeling approach

There are now a large number of efficiency models which differ in their detail and complexity, but all are based on the idea that knowledge of incident radiation and light-absorbing properties of the plant canopy can determine the maximum potential photosynthesis for that canopy. The models which use the LUE approach can be categorized as production efficiency model (PEM) or a light-use efficiency (LUE) model. Each group has different strategies adopted by each model. According to (Ruimy et al., 1999, Cramer et al., 1999b), production efficiency models were identified as CASA, GLO-PEM, TURC and SDBM all of them derived NPP at global scale level. The light use efficiency model has been used to estimate GPP and net primary production (NPP) at various spatial and temporal scales.

2.2.1 LUE (Light Use Efficiency) model

Predicting the gross primary productivity (GPP) of terrestrial ecosystems has been a major challenge in quantifying the global carbon cycle (Canadell et al., 2000). Among all the predictive methods, the light use efficiency (LUE) model may have the most potential to adequately address the spatial and temporal dynamics of GPP because of its theoretical basis and practicality (Running et al., 2000). Light-use efficiency (LUE) approach is a concept used for NPP estimation and was explored by Monteith (1972, 1977). Now days this approach has been used in many models to estimate carbon uptake by vegetation. The light-use efficiency (LUE) approach is widely used to estimate NPP at large scales because it is conceptually simple and can be directly parameterized with remote sensing data (Ahl et al., 2005, Gower et al., 1999). According to Gower et al. (1999), the LUE approach has two advantages, namely 1) it is simple and some evidence exists to suggest that maximum light use efficiency may be conservative within major vegetation classes. 2) The fraction of photosynthetically active radiation absorbed by green leaves in a canopy (*f*APAR) can be remotely sensed, as has been shown in both empirical (Daughtry et al., 1992, Landsberg and Waring, 1997) and theoretical studies (Myneni et al., 1995).

The light use efficiency model described here is the concept used by Turner et al. (2005) for estimating GPP and NPP respectively. The specific components of the algorithm that produces the NPP/GPP products include climate and satellite-based inputs as well as a look-up table for biome-specific parameters related to photosynthesis and autotrophic respiration. The components of the model NPP/GPP algorithm are described by Running et al. (2000). Gross primary production is derived on daily basis as:

$$GPP = \downarrow PAR \times fPAR \times (\varepsilon_{g\text{-}max} \times S_{Tmin} \times S_{VPD}), \tag{1}$$

where GPP is gross primary production (gC m^{-2}day^{-1}), $\downarrow$PAR is incoming photosynthetically active radiation (Wm^{-2} or MJ m^{-2}), fPAR is fraction of $\downarrow$PAR absorbed by the plant canopy, $\varepsilon_{g\text{-}max}$ is maximum light use efficiency (gC MJ^{-1}), S_{Tmin} is minimum temperature scalar (0 −1), and S_{VPD} is vapor pressure deficit scalar (0 −1).

Net primary production is derived on daily basis and next on annual basis as the total daily net primary production.

$$NPP_{daily} = GPP - R_a, \tag{2}$$

$$R_a = R_m + R_g \tag{3}$$

$$NPP_{Annual} = \sum_{i=1}^{365} NPP_{daily} \tag{4}$$

where NPP is net primary production (gC m^{-2}day^{-1}), R_a is autotrophic respiration (gC m^{-2}day^{-1}), R_m is maintenance respiration (gC m^{-2}day^{-1}), a function of biomass (derived from LAI) and temperature, summed across biomass compartments, and R_g is growth respiration (gC m^{-2}day^{-1}), a function of biomass growth, summed across biomass compartments.

2.2.2 CASA (Carnegie-Ames-Stanford-Approach) model

The CASA (Carnegie-Ames-Stanford-Approach) model is a production efficiency model introduced by (Potter et al., 1993). This model estimates NPP based on the LUE approach. It uses a combination of ecological principles, satellite data, and surface data to predict terrestrial NPP on a monthly time step. This model is driven by satellite data as well as by temperature, precipitation, solar radiation, land cover and soil classifications (Hicke et al., 2002). CASA computes NPP as a function of the absorbed photosynthetically active radiation (APAR), a maximum potential light-use efficiency variable ε, temperature (Ts) and moisture (Ws) scalars that represent climate stresses on vegetation light-use efficiency. The CASA model incorporates a structure that allows LUE to vary seasonally. The potential LUE value is empirically derived, and may be reduced by environmental constraints (Field et al., 1995). The CASA model estimates NPP for each time step as:

$$NPP = \sum PAR * fAPAR * \varepsilon * \Delta t \tag{5}$$

where PAR is the total incident photosynthetically active radiation (MJ), fAPAR the fraction of PAR absorbed by photosynthetic tissues (unitless), ε the light use efficiency (LUE) (g MJ^{-1}PAR), and the summation is taken over the growing season.

Light use efficiency ε is calculated as the product of an optimal ε* and its temperature and water stressors (Tao et al., 2005) as stated below:

$$\varepsilon = \varepsilon^* \, T1 \, T2 \, Ws \tag{6}$$

where ε* is the global maximum light use efficiency for above-ground biomass when the environmental conditions are optimal, and T1, T2 and Ws are scalars representing environmental stressors that reduces LUE (Field et al., 1995).

2.2.3 GLO-PEM (Global Production Efficiency Model) model

GLO-PEM was developed to simulate GPP and NPP over large areas using algorithms driven entirely with remotely sensed measurements. This model is a semi-mechanistic plant photosynthesis and respiration model driven entirely with satellite observation from the Advanced Very High Resolution Radiometer (AVHRR). The GLO-PEM approach developed by Prince and Goward (1995) was the first attempt to model both global net and gross primary production using satellite data to measure both absorption of photosynthetically active radiation (APAR) and also environmental variables that affect APAR in primary production. The model estimates a wide range of biophysical variables at 10-day intervals including air temperature, vapor pressure deficit, soil moisture, biomass, autotrophic respiration, canopy-absorbed photosynthetically active radiation, gross primary production, and light use efficiency (Goetz et al., 2000). According to Prince and Goward (1995) GLO-PEM is unique in its use of visible, near-infrared and thermal channels of the AVHRR to obtain continuous fields of driving variables (e.g., air temperature, humidity, canopy light absorption) rather than using the sparse network of meteorological stations or coarse resolution climate model results. The model is also referred to as a mechanistic model of primary production which uses variables that can be remotely sensed at a global scale (Goetz et al., 1999). The model in its simplest form is summarized as follows:

$$NPP = \sum_t [(\sigma_t LUE^* g_t)(fAPAR^* PAR) Y_g Y_m] \tag{7}$$

Where σ_t is the reduction factor due to environmental stressors in time interval t (a proportion), $LUE^* g_t$ is the potential LUE in terms of gross production (gC MJ^{-1}), it is identified with the quantum yield of a leaf, a well-known variable with defined values and dependency on particular biochemical carbon fixation pathway and temperature, fAPAR the fraction of incident photosynthetic active radiation (PAR) absorbed by the canopy and Y_g, Y_m are measures of respiration.

2.2.4 TURC (Terrestrial Uptake and Release of Carbon) model

The terrestrial uptake and release of carbon (TURC) approach, is a diagnostic model for the estimation of continental GPP and NPP (Ruimy et al., 1996). TURC computes NPP as the difference between photosynthesis (i.e. gross primary productivity GPP) and carbon released by autotrophic respiration (Ra). Time varying inputs of the model are the incoming solar radiation (300-4000 nm), air and soil temperature and satellite vegetation index (NDVI). Normalized difference vegetation index (NDVI) is used to estimate the fraction of incoming photosynthetically active radiation (fPAR) that is absorbed by vegetation and leaf biomass. This model uses meteorological forcings (air temperature, incoming solar radiation), together with satellite observations (Normalized Difference Vegetation Index, NDVI) and a map of

ecosystem biomass. For the maintenance respiration, different plant organs are distinguished: leaves, fine roots and wood (Lafont et al., 2002). TURC assume one constant light-use efficiency (LUE) value for the estimation of the GPP, and applied environmental constraints on the estimation autotrophic respiration (R_a). According to Ruimy et al. (1996) TURC model is used the concept of Monteith (1972, 1977) which defined NPP as the product of incident solar radiation by several factors, or efficiencies:

$$P_n = \varepsilon * f * c * S_g \tag{8}$$

where P_n is net primary productivity, ε is the efficiency of conversion of absorbed PAR into dry matter or "conversion efficiency", f is the efficiency of radiation absorption by the canopy or "absorption efficiency"; c is the ratio of incident photosynthetically active radiation (PAR), S_g is climatic efficiency. Also f has been related to vegetation indices calculated from reflectances in the red and near-infrared channels of NOAA-advanced very high resolution radiometer (AVHRR).

2.2.5 SDBM (Simple Diagnostic Biosphere Model) model

The Simple Diagnostic Biosphere Model (SDBM) uses the satellite-derived normalized-difference vegetation index (NDVI) to calculate the photosynthetically active radiation absorbed by the canopy. Knorr and Heimann (1995) calibrated SDBM in two steps. First, they determined two global parameters, the light-use efficiency in NPP and the temperature sensitivity of heterotrophic respiration (R_H) to match the seasonal atmospheric CO_2 signal at five northern monitoring stations. Land use is implicitly considered in SDBM, since it is based on NDVI. SDBM considered a potential LUE, which is reduced by a drought factor (AET/PET) (Nemry et al., 1999). The calculation is performed on the basis of measured Normalized Differential Vegetation Index (NDVI), incoming solar radiation, and surface temperature.

2.2.6 Model comparison

Production efficiency models (PEMs) and LUE model both use a light-use efficiency approach to estimate NPP. These models are distinguished according to their strategies adopted in the NPP estimation. The strategies can be summarized as spatial and temporal resolution of the input data used, scale level applicable, use of biophysical factors or climate variables and ways of processing. Table 1 below indicates the comparison between production efficiency models and light use efficiency model.

Table 1 Comparison of characteristics for production efficiency models and light use efficiency model

NA.	Production efficiency models (PEM)	Light-use efficiency model
1.	Applied at global scale level	Applied at local/regional and global scale level
2.	Used input data (applicable) at coarse spatial resolution	Used input data (applicable) at fine spatial resolution
3.	Generate GPP/NPP at coarse temporal resolution (e.g. 10days, monthly)	Generate GPP/NPP at fine temporal resolution (daily).
4	Used meteorological data (applicable) at coarse scale	Use local meteorological data (applicable) at fine scale
5	Model utilizes variables retrieved entirely with remotely sensed observations including environmental factors (e.g. temperature)	Model utilized variable retried from both remote sensing and in-situ data

Regarding to the objective of the research, several criteria were identified and used to evaluate the appropriate model in this study. The identified research requirements are 1) model should be able to generate GPP/NPP on daily basis 2) model should be capable of estimating GPP/NPP at large scale 3) model should be applied at local scale level 4) model should generate GPP/NPP separately, and 5) restriction in the data availability was also taken into consideration. Based on these requirements, each model characteristics was explored and compare for the best fit to the requirements. Light-use efficiency model seems to be more appropriate for better estimation of GPP/NPP in this study. This is because of its ability to utilize large spatial and temporal data, generate GPP/NPP on daily basis, applied the model at local scale level, and the ability to handle the integration of in-situ data of fine resolution and remote sensing data with varied scale. Table 2 below describe in detailed on the strategies for calculating GPP/NPP (Cramer et al., 1999a, Running et al., 2000).

Table 2 Spatial and temporal variation in different models for estimation GPP/NPP

Model	Full name	Spatial resolution of NPP	Temporal resolution of NPP	NPP calculated as:	Model parameters	No. of VEGC pools	strategy
CASA	Carnegie-Ames-Stanford-Approach model	$1° \times 1°$	1 month	NPP	NPP = f(SRad, FPAR, Temp, AET/PET)	0	PEM, LUE derived empirically, applied to NPP
GLO-PEM	Global Production Efficiency model	8km x 8km	10 days	GPP- R_A	GPP = f(SRad, FPAR, Temp, SW, VPD) R_A = f(VegC, GPP)	2	PEM, LUE derived from mechanistic model, applied to GPP
TURC	Terrestrial Uptake and Release of Carbon Model	$1° \times 1°$	1 month	GPP- R_A	GPP = f(SRad, FPAR) R_A = f(VegC, Temp)	3	PEM, LUE derived empirically (global value), applied to GPP, environmental constraints applied to R_A
SDBM	Simple Diagnostic Biosphere Model	$0.5° \times 0.5°$	1 month	NPP	NPP = f(SRad, FPAR, CO_2)	4	PEM, LUE derived empirically, applied to NPP
LUE	Light-Use Efficiency	Both large and small spatial resolution	daily	GPP- R_A	GPP= (Fpar, PAR, ε, Temp, VPD) R_A = Rm + Rg	3	

Note: SRad is solar radiation, SW is soil water, VPD is vapour pressure deficit, Ra is autotrophic respiration, AET is actual evapotranspiration, PET is potential evapotranspiration, Rm is maintenance respiration, Rg is growth respiration and **ε is** conversion efficiency.

2.3   LUE model input and parameterization

In the LUE model, the processes of gross primary production (GPP) and autotrophic respiration (Ra) are treated separately. Each input parameters used to generate gross primary production (GPP) and net primary production (NPP) is also derived separately. The parameterization of individual variable in the equations has been reviewed in the following sections.

2.3.1 Fraction of photosynthesis active radiation

According to (Running et al., 2000, Running et al., 2004), the fraction of photosynthetically active radiation (fPAR) can be estimated from remote sensing data. Spectral vegetation indices derived from remotely sensed data have several forms, the most widely used currently is the normalized different vegetation index (NDVI) which uses reflectance from red and near-infrared (NIR) wavelengths as:

$$NDVI = \frac{NIR - RED}{NIR + RED}$$
(9)

A spectral vegetation indexes such as NDVI (ranging from 0 to 1) can be used as an estimate for fPAR (Prince and Goward, 1995):

$$fPAR \approx NDVI$$
(10)

According to (Prince and Goward, 1995) the spectral vegetation index measurements produced by calculating the NDVI have shown, empirically and theoretically, to be related to the fraction of incident PAR absorbed (*fPAR*) in vegetation canopies.

Alternatively, fPAR can be derived from leaf area index (LAI). According to (Turner et al., 2003) the conversion of the ground-based LAI to fPAR used a simple Beer's Law approach (Jarvis & Leverez, 1983).

$$fPAR = 1 - (e^{(LAI*(-k))})$$
(11)

where k is the canopy light extinction coefficient. This approach requires a reliable estimation of k, which is mainly related to leaf optical properties, distribution, and orientation. The canopy extinction coefficient is determined by the angle distribution of leaves in the canopy and the incidence angle of the radiation. The equation describing this is:

$$k = \frac{\sqrt{x^2 + \tan^2 \theta}}{x + 1.744(x + 1.182)^{-0.733}}$$
(12)

where x is the leaf angle distribution parameter and θ is the angle of incidence of the radiation.

2.3.2 Photosynthetic active radiation

Plants require solar radiation for photosynthesis, and their growth rate is proportional to the amount received. Photosynthetically active radiation ($\downarrow$PAR) consists of wavelengths utilized by the plant biochemical processes in photosynthesis to convert light energy into biomass.

The PAR can be defined as quantum units of light energy, and expressed as the number of photons of light received on a unit area (Kania and Giacomelli, 2005). When measuring light by quanta (or number of photons), the common unit reported is micromoles per second per square meter ($\mu mol\ s^{-1}\ m^{-2}$). This is an instantaneous rate, and is measured by a quantum sensor for example every 15 minutes. The fraction of PAR absorbed by the plant canopy is an essential parameter relating the available visible solar radiation to its absorption by the chlorophyll for plant photosynthesis. PAR data is normally obtained from a meteorological station. Instantaneous PAR is very useful for NPP estimation, but the LUE model requires a daily time step and thus instantaneous data must be integrated.

The PAR also can be estimated from the incidence shortwave radiation. It has been assumed in various applications that incident PAR is half of the incident shortwave radiation (insolation) that is routinely measured at weather stations. However, several studies indicated that this ratio is not constant in time. Jacovides et al. (2003) found that this ratio varied between 0.460 and 0.501 in hourly measured values. The conversion factor varies seasonally and by geographical location on Earth. For example Pinker et al. (1995) found a factor of 0.45 best approximates the PAR fraction in shortwave radiation for the eastern United States.

2.3.3 Maximum conversion efficiency

Maximum light-use efficiency ($\varepsilon_{g\text{-}max}$) is a key parameter for estimation of net primary productivity (NPP). Estimation of NPP from LUE models may be improved if vegetation specific $\varepsilon_{g\text{-}max}$ values are used (Goetz and Prince, 1999). The maximum light use efficiency or conversion efficiency varies widely with different vegetation types (Prince and Goward, 1995). According to Running et. al. (2000), there are two principal sources of this variability. First, with any vegetation, some photosynthesis is immediately used for maintenance respiration. Running and Hunt (1993) and Hunt (1994) hypothesized that lower $\varepsilon_{g\text{-}max}$ values for woody vegetation (0.2 to 1.5 $gCMJ^{-1}$), is the result of respiration from the living cells in the sapwood of woody stems. The second source of variability in $\varepsilon_{g\text{-}max}$ is due to suboptimal climate conditions.

Various publications have documented the derived values of $\varepsilon_{g\text{-}max}$ per land use type (Ahl et al., 2004), other individual studies have suggested factors such as stand age, species composition, soil fertility, and foliar nutrients (Gower et al., 1999). Information about $\varepsilon_{g\text{-}max}$ for individual vegetation types can be obtained from a survey of the literature for example the $\varepsilon_{g\text{-}max}$ values as published by (Gower et al., 1999, Ahl et al., 2004). Table 3 below is an example of the derived values of $\varepsilon_{g\text{-}max}$ per land use type extracted from (Ahl et al., 2005).

Table 3 Conversion efficiency per land-use type

Land use	Conversion efficiency (gC/MJ)
Forested wetland	0.41
Forest	0.53
Wetland	0.27
Grassland	0.30
Cropland	3.0

This retrieved $\varepsilon_{g\text{-}max}$ applied to a maximum value established for each vegetation type is attenuated by two controls. These controls are
- Stomatal closure due to cold night temperature (TMIN) and

- Stomatal control due to daytime vapour pressure deficiency (VPD)

The two parameters for TMIN and the two parameters for VPD are used to calculate two scalars that attenuate $\varepsilon_{g\text{-}max}$ to produce the final conversion efficiency (ε) used to predict GPP.

Photochemical Reflectance Index

The photochemical reflectance index (PRI), derived from narrow band reflectance at 531 and 570 nm has been related with some success to photosynthetic light-use efficiency (LUE). The photochemical reflectance index (PRI) is a reflectance measurement that is sensitive to changes in the carotenoid pigments (particularly xanthophyll pigments) in living foliage. Carotenoid pigments are indicative of photosynthetic light use efficiency, or the rate of carbon dioxide uptake by foliage per unit energy absorbed (Gamon et al., 1992, Gamon et al., 1997). Recent studies have shown that the photochemical reflectance index (PRI), derived from narrow waveband reflectance at 531 and 570 nm, can be used as a remote measure of photosynthetic light-use efficiency (LUE). Previous studies have shown that the relationship between the PRI and LUE can be used to estimate photosynthetic performance at both leaf and canopy scales (Gamon et al., 1992). The relationship between vegetation reflectance at 531 nm and photosynthetic light-use efficiency (LUE) has been studied for leaf and small vegetation plots showing that the PRI provides a widely applicable index of vegetation LUE across species, functional types, and nutrition levels (Gamon et al., 1997). According to Gamon et al. (1992), PRI tracks both diurnal and seasonal variation in photosynthetic activity. The PRI is defined by the following equation:

$$PRI = \frac{\rho_{531} - \rho_{570}}{\rho_{531} + \rho_{570}} \qquad (13)$$

where ρ_{531} indicates reflectance at 531nm (the waveband of the "xanthophyll signal"), and ρ_{570} indicates the reflectance at 570nm (a reference waveband) (Gamon et al., 1992).

PRI has been correlated with both the epoxidation state of the xanthophyll cycle pigments and LUE in several field studies at the leaf and ecosystem levels (Gamon et al., 1992). Correlations between PRI and ecosystem LUE were recently found when PRI was obtained from hyperspectral data acquired by aircraft (Rahman et al., 2001). More recently, (Rahman et al., 2004) used MODIS reflectance data from bands originally intended for ocean observations and calculated PRI over a temperate deciduous forest. Rahman et al. (2004) was estimating "continuous field" LUE of terrestrial vegetation using the MODIS ocean bands #11 (bandwidth 526-536 nm) and #12 (546-556 nm) over a forested terrestrial ecosystem, in which all requisite data are obtained directly from satellite sensors. They found a high correlation of MODIS-PRI with daily NPP that was derived from Eddy Covariance data (Guillaume et al., 2005).

2.3.4 Temperature

Temperature measurements for NPP estimation are obtained from meteorological stations and have been separated as minimum air temperature and mean air temperature. Both minimum and mean air temperature are instantaneous measurements and are measured for example, every hour.

2.3.5 Vapor pressure deficit

Vapor Pressure Deficit (VPD) is the difference (deficit) between the amount of moisture in the air and how much moisture the air can hold when it is saturated. For plants to preserve essential moisture, stomata respond to the relative difference between the vapor pressure (a measure of the amount of water) inside a leaf and that of the outside air. This difference in vapor pressure inside and outside a leaf is termed the vapor pressure deficit (VPD). It is an index of the drying capacity of the air, and it varies with temperature and humidity conditions. VPD strongly affects photosynthetic rates. In dry conditions, leaves may be unable to maintain adequate moisture and respond by closing stomatal pores. Stomatal closure restricts not only the diffusion of water out of the leaf but also carbon dioxide diffusion into the leaf, resulting in reduced photosynthesis. Plants respond differently to VPD depending on the environment to which they have adapted.

VPD can be estimated using an online VPD calculator with input requirements as mean air temperature and relative humidity (http://www.autogrow.com/1_information/1_vpd/info_vpd.html) or using the following formulas (14 – 16). To compute the VPD we need the ambient (greenhouse) air temperature, the relative humidity and if possible, the canopy air temperature (Wikipedia).

- Calculate the saturation vapor pressure of the air (VP_{sat})

$$VPsat = 0.61365e^{\frac{17.502*T}{240.97+T}}$$
(14)

where $VPsat$ is saturation vapor pressure (kPa) and T is average temperature (ºC). The above equation can be find from the following link; http://www.licor.com/env/Products/li6400/6400_manuals.jsp click on "instruction manual" and go to book 3 pg 14-10.

- Calculate the VP_{sat} of the canopy: Same as above, T – Temperature of the canopy in ºK . If canopy temperature is unknown, proceed to step below.

- Calculate vapor pressure in the air (VP_{air}) at the actual relative humidity.

$$VP_{air} = VP_{sat} * \text{relative humidity}$$
(15)

- Calculate VPD as difference between saturation vapor pressure and vapor pressure in the air.

$$VPD = VP_{sat} - VP_{air}$$
(16)

Or $$VPD = VP_{\text{canopy sat}} - VP_{air}$$
(17)

2.3.6 Autotrophic respiration

In the user guide of MOD17A2/MOD17A3 Heinsch et al. (2003) has describe in detail an algorithm to derive autotrophic respiration, R_a. In their method, the maintenance respiration (R_m) and growth respiration (R_g) components are derived from allometric relationships which have been developed from an extensive literature review, and incorporate the same parameters

as those used in the BIOME-BGC ecosystem process model (White et al., 2000). Therefore, autotrophic respiration is estimated as the sum of maintenance respiration, R_m, from the three live vegetation components (leaves, stem, and root) and growth respiration, R_g.

$$R_a = R_m + R_g \qquad (18)$$

Recently, Tao et al. (2005) used a simple approach in the estimation of autotrophic respiration. In their work, the autotrophic growth respiration is expressed as 25% of the GPP while maintenance respiration algorithm is modeled using a semi-empirical relationship with standing above ground biomass (W, Mg m^{-2}). Above-ground biomass was estimated based on the following expression;

$$W = 7166.1(\rho_{min}^{-2.6}) \qquad (19)$$

where W is the above-ground standing biomass (Mg m^{-2}), and ρ is the minimum reflectance (ρ_{min}, %) in AVHRR channel 1. According to Tao et al. (2005), maintenance respiration can be estimated based on biomass and the deviation of T from climatological air temperature Tc.

$$R_m = 0.53 * (\frac{W}{W + 50}) * e^{0.5}(\frac{Tc - T}{25}) \qquad (20)$$

where Tc is the base temperature and is constant at 25ºC, and T is the daily average temperature. Therefore, the approach used by Tao et al. (2005) in the estimation of autotrophic respiration was adopted in this thesis.

3 MATERIALS AND METHODS

3.1 *Study area*

The study area is located within the polder of Gendt which is along the Waal near the city of Nijmegen. It covers approximately an area of 25 km^2. The area is north of river Waal, about 7 kilometers east from Nijmegen. The nearest node in the sensor web is located at 51°52´16.88´´N and 5°56´42.79´´E. According to weather station (KNMI, 2003-2004) the temperature variation ranges between -10.6 minimum and 35 maximum per year and the annual precipitation ranges between 750 and 775mm. This area is prone to flooding risks when water levels in the river are high. This situation leads to seepage through dikes and the land in the polder may become flooded (Abdi et al., 2007). Figure 3 is an aerial photograph of the study area.

Figure 1 Arial photograph of the study area, which is indicated in red

3.2 *Data*

3.2.1 Remote sensing data

In this thesis a Dutch land use database (LGN4) dataset was used. The LGN4 dataset is a Dutch land use database and it is based on satellite imagery from 2003 and 2004 and additional data. The nomenclature of the database includes crop types, forest types, water, various urban classes and several ecological classes. Satellite imagery for LGN4 is a combination of Landsat ETM7 and TM5, LISS-1c and ERS-SAR images. According to (Hazeu, 2006) the images were georeferenced and cubic convolution was used to resample the images to 25m grid size.

3.2.2 Sensor web data

Within the study area, in-situ measurements are being collected by a set of sensors and the acquired data are distributed to users for different applications. These data are available to Wageningen University who participate in a team which is involved in a RGI (Space for Geo-information) project called "Sensor as a data source". Minimum and mean air temperature,

photosynthetic active radiation (PAR), and relative humidity are examples of meteorological data that were required in this research.

However, an examination of the first data delivered by the sensors revealed that the radiance and relative humidity sensors were mal-functioning. Therefore, an alternative time series of meteorological data from the Haarweg location in Wageningen was chosen. At this location there is no direct measurement data available for PAR. Therefore, this was estimated from the measurement of the shortwave incoming radiance (Wm^{-2}) which is collected every hour. The air temperature dataset used in the estimation of VPD was from the Gendt and Haarweg weather stations. Data from January to June was from Haarweg and July till December was from Gendt. Because of some limitation in the availability of data from June to December, a nearby weather station was used as an alternative.

3.2.3 Surface reflectance product

MOD09 GQ is a MODIS/Terra surface reflectance product which provides band 1(range 620-670 nm) and band 2 (range 841-876 nm) at 250-meter resolution in a daily gridded L2G product in the Sinusoidal projection. The surface reflectance product is a major input utilized in the generation of several land products: vegetation indices, BRDF, land cover, snow cover, thermal anomalies, and LAI/fPAR. For the purpose of this research the product was used to generate NDVI (normalized difference vegetation index).

3.2.4 MODIS 8 days GPP product

MOD17A2 is an 8-day composite at 1-kilometer spatial resolution provided as a gridded level-4 product in the Sinusoidal projection. This product produces gross primary production of vegetation every day, and sums to net primary production, essentially vegetation growth, at the end of the year. The product is computed with daily MODIS land cover, FPAR/LAI and global GMAO surface meteorology at 1km for the global vegetated land surface. This product provides an accurate measure of terrestrial vegetation growth and production activity. The product can be searched and ordered via the following web link http://edcimswww.cr.usgs.gov/pub/imswelcome/.

3.2.5 MODIS annual NPP product

MOD17A3 is an Annual Net Primary Productivity product. The vegetation production product is designed to provide an accurate regular measure of the growth of the terrestrial vegetation. This product produces gross primary production of vegetation every day, and sums to net primary production, essentially vegetation growth, at the end of the year. The product is computed with daily MODIS land cover, FPAR/LAI and global GMAO surface meteorology at 1km for the global vegetated land surface. These variables provide the initial calculation for growing season and carbon cycle analysis, and are used for agriculture, range and forest production estimates.

Spatially, MODIS has a much coarser resolution than some other satellite sensors (1km x 1km). Data from MODIS are well-suited to large regional or global analyses. Temporally, MODIS is much better than many satellite sensors, with its daily overpasses and 8-day compositing of the data, which can be used to look at annual productivity and inter-annual variability of both GPP and NPP. There is no other satellite that can provide a global, 8-day look at vegetative productivity and carbon balance on an annual basis. In addition, these data are available in near-real time, which will allow users to make comparisons with their own

research data during the growing season, often within weeks of the actual data collection. Periodic reprocessing of the data will allow for interpolation of missing data, resulting in a more complete, and more accurate product (Heinsch et al., 2003). MOD17A3 product can be searched and ordered via the web link http://edcimswww.cr.usgs.gov/pub/imswelcome/.

3.3   Data integration conceptual model

Several literature sources have published different methods for data integration to estimate NPP over large area. However, this thesis intends to integrate data from different sources to estimate NPP over a small area. The thesis aims to adapt a light use efficiency model in the estimation of NPP. Figure 4 summarizes the approach used for data integration in a light use efficiency model to estimate daily GPP and NPP. This conceptual model also included the comparison of MODIS products (MOD17A2/3) with the derived GPP/NPP.
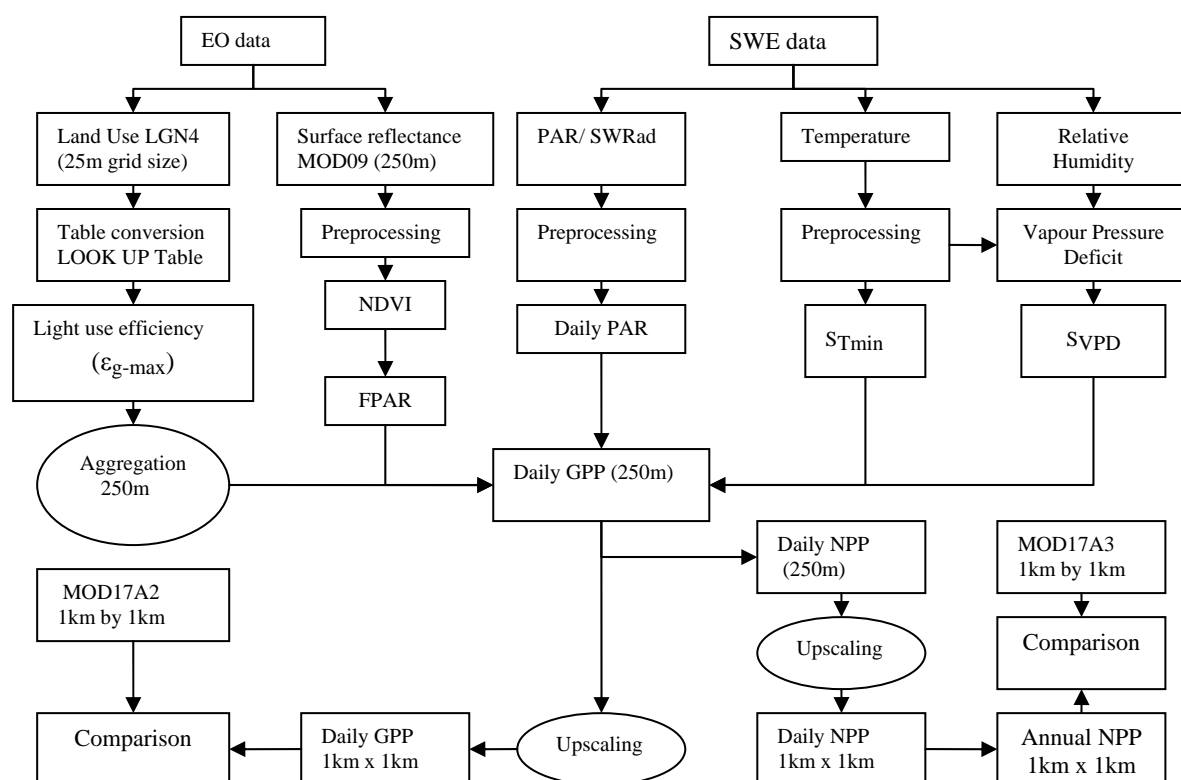
Figure 2 Conceptual model indicates connection in research strategies for NPP estimation

3.4   Preprocessing of meteorological data - Instantaneous temporal Scaling

The term scaling refers to data, processes, or models. Scaling addresses the process of translating information from one scale to another. It requires the definition of a source and a target scale including grain and extent. Scaling from small to large scale is called up-scaling, in the other direction downscaling. Up-scaling and downscaling are also referred to as "aggregation" and "disaggregation" respectively. Scaling is needed for a variety of reasons. One is incompatibility of data gathered at different scales. To make such data compatible, they must be transformed to a common target scale. Scaling is also necessary to translate model processes from one to another scale. For example, the lack of small scale data or

17

restricted computing resources can impede large scale model simulations. Then the model's process functions or the data should be adapted to the coarser scale.

Many of the available meteorological data varies in temporal scale. The LUE model as proposed for this study requires a daily time step to derive GPP productivity. Preprocessing of meteorological data based on temporal scaling is an important step in this research in order to harmonize the available datasets that were available on a hourly basis and adapted to a daily basis as model input requirement. Similarly, some meteorological datasets are not directly used as input into the model rather they need to be either averaged or integrated or combined with others dataset to derive the input variables for the model. Therefore, processing is considered as a necessary and important step for this research. Temporal scaling was done to the following meteorological datasets; photosynthetic active radiation (PAR), air temperature and relative humidity.

3.4.1 Daily photosynthetic active radiation

PAR is an instantaneous flux measurement and is very useful for NPP estimation, but many models (e.g. the LUE model) requires a daily time step and thus the daily PAR product is more desirable. The daily PAR was estimated based on shortwave radiations which were measured on a hourly basis by the sensor. A conversion factor of 0.45 was used to convert shortwave radiation to PAR. This factor has been reported in different literature sources as suitable for conversion purpose (Pinker et al., 1995). The unit for shortwave radiation from the data provider is Wm^{-2} and was converted to $MJ\ m^{-2}$ to comply with the input model unit. Hourly shortwave radiation measurements were converted into PAR and integrated into daily basis as expressed below.

$$PAR_{daily} = \sum_{i}^{n} (\text{SWRad} * 0.45) * 3600 / 10^{6} \tag{21}$$

Where PAR_{daily} is the daily PAR ($MJ\ m^{-2}$), SWRad in the incoming shortwave radiation (Wm^{-2}), and n is the number of measurements over a day.

3.4.2 Daily minimum temperature scalar

Light use efficiency model requires scalar values (0 – 1) for minimum temperature as input in the model. Therefore, the available minimum temperature from meteorological data can not be used as direct input in that model. Minimum temperature scalar was estimated based on simple linear ramp functions as presented in Figure 3. The values for $TMIN_{min}$ and $TMIN_{max}$ per land use type were extracted from the look up table compiled by Heinsch etal., 2003 as presented in table 4.
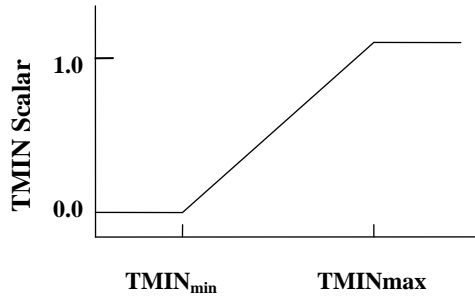
Figure 3 Simple linear ramp function for STmin estimation

where $TMIN_{min}$ (ºC) is the daily minimum temperature at which $\varepsilon = 0.0$ and $TMIN_{max}$ (ºC) is the daily minimum temperature at which $\varepsilon = \varepsilon_{max.}$ When TMIN scalar >1, then TMIN scalar =1 assuming that no influence on vegetation growth similarly, when TMIN scalar < 0, then TMIN scalar = 0 also no vegetation growth taking place.

The scalar values for the measured minimum temperature (Tmin) were derived as follows; if Tmin is lower than TMINmin then scalar value is 0 or if Tmin is higher than TMINmax then scalar value is 1, otherwise a simple mathematical expression was used:

$$ST\min = \frac{T\min - TMIN\min}{TMIN\max - TMIN\min} \tag{22}$$

where STmin is the scalar value for minimum temperature range between 0 and 1. Table 4 below summarized the extracted values of TMINmin, TMINmax, VPDmin and VPDmax per land use type. These values were extracted from a look up table as compiled by Heinsch et al. (2003).

Table 4 Values for daily TMINmin, TMINmax, VPDmin, VPDmax per land use type

Land use type (LU)	TMINmin(ºC)	TMINmax(ºC)	VPDmin(Pa)	VPDmax(Pa)	Source
Grassland	-8	12.02	650	3500	Heinsch etal., 2003
Cropland	-8	12.02	650	4100	Heinsch etal., 2003
Mixed forest	-8	8.5	650	2500	Heinsch etal., 2003
Deciduous broadleaf forest	-8	7.94	650	2500	Heinsch etal., 2003
Open wetland/ open shrubland	-8	8.8	650	3600	Heinsch etal., 2003
Natural herbaceous vegetation	-8	12.02	650	3500	Heinsch etal., 2003

3.4.3 Daily vapour pressure deficit scalar

The daily vapor pressure deficit scalar is derived from daily VPD. This VPD is estimated from daily average relative humidity and air temperature. Relative humidity and air temperature are meteorological datasets which are collected in every one hour. Therefore, relative humidity and air temperature were averaged into daily basis in order to derive daily VPD. The average of both air temperature and relative humidity was based on simple expression as illustrated below.

$$T_{avg} = \frac{1}{N}\sum_{i=1}^{n}T_i \tag{23}$$

where T_{avg} is average temperature (ºC) over a day, T_i is instantaneous temperatures measured at every moment of time (e.g. 60minutes) and n is the number of observations over a day.

The average air temperature was used in equation 14 to derive *VPsat*, average relative humidity was applied in equation 15 to derive *VPair* and finally VPD was derived based on equation 16. The VPD scalar value was estimated based on simple linear ramp functions. Figure 4 illustrate the simple linear function used to estimate daily vapour pressure scalar. The values for VPD_{min} and VPD_{max} per land use type were extracted in a look up table as compiled by Heinsch et al. (2003).
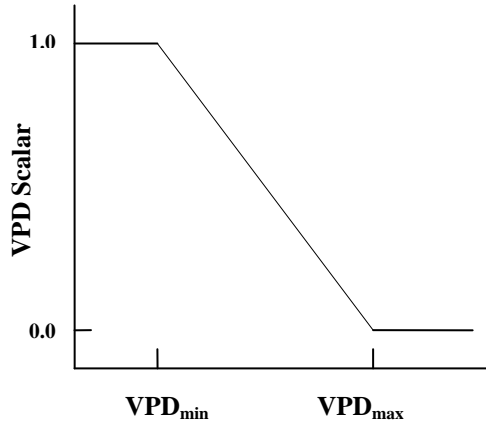
Figure 4 Simple linear ramp function for S_{VPD} estimation

Where VPD_{min} (Pa) is the daylight average vapor pressure deficit at which $\varepsilon = 0.0$ and VPD_{max} (Pa) is the daylight average vapor pressure deficit at which $\varepsilon = \varepsilon_{max}$. When VPD_{min} scalar >1, then VPD_{min} scalar =1 there is no influence on vegetation growth also when VPD_{max} scalar < 0, then VPD_{max} scalar = 0, no vegetation growth taking place.

The scalar values for the estimated VPD is derived based on the following assumption. If VPD is lower than VPD_{min} then scalar value is 1 or if VPD is higher than VPD_{max} then scalar value is 0, otherwise a simple mathematical expression was applied as follows.

$$Svpd = 1 - \left(\frac{VPD - VPD\min}{VPD\max - VPD\min} \right) \tag{24}$$

Where *Svpd* is the scalar value for vapour pressure deficit range between 0 and 1.

3.5   Processing – Modelling of GPP and NPP

Figure 5 below indicates the structure/flowchart of the entire LUE model implementation. It indicates how remote sensing and sensor web data were integrated. Different software's were used in the implementation of the model such as ArcMap, Erdas Imagine, and Modis Reprojection Tool (MRT). The output of this model is the time series daily GPP, time series daily NPP and annual NPP.

Sensorweb data

Temperature (ºC)

Relative Humidity (%)

SWRad (Wm^{-2})

Daily Tmin — Preprocessing — Daily Tavg — Preprocessing

Preprocessing

Daily PAR (MJm^{-2})

S_{Tmin} per LU type

Light use efficiency (ε_{g-max}) per LU type

S_{VPD} per LU type

VPD

LGN4 (25m) 20 classes

MOD09(250m) HDF- format

Reclassify LGN4 7 classes (LU) (ARCMAP)

Aggregate (250m) per classes (LU) (ARCMAP)

(ε_{g-max} * S_{Tmin} * S_{VPD}) EXCEL

MRT

MOD09(250m) UTM-Tiff format

LU * ε ARCMAP

Time series Daily GPP (250m) ARCMAP

NDVI - (250m) ERDAS IMAGINE

Time series Daily NPP GPP – Ra ARCMAP

Autotrophic respiration (Ra) Rm + Rg ARCMAP

Maintenance respiration Rm ERDAS IMAGINE

Annual NPP ARCMAP

Growth respiration Rg ARCMAP

Figure 5 LUE model implementation

3.5.1 Aggregation of land Use classes

Spatial scaling was considered as an important step during model implementation in this thesis. Since model implementation involved integration of different datasets, transformation of those data to a common target output scale is inevitable at this stage. For example, LGN4 and surface reflectance are datasets incompatible in spatial scaling namely 25m and 250m respectively. But these datasets needs to be integrated for the purpose of generating GPP. Upscaling of LGN4 from 25m to 250m was performed during model implementation at a stage where scaling compatibility was necessary. Before the aggregation process is applied, reclassification of LGN4 was performed based on seven lasses rather than original twenty classes. The reclassification is intended to combine a particular land use class together such as crops and forests. The classified seven classes are grassland, cropland, mixed forest, deciduous forest, open wetland and natural herbaceous vegetation and urban.

Aggregation technique
The aggregate technique theoretically just aggregates a series of cells to the same value to produce a single, coarser resolution cell. The aggregate function resamples an input raster to a

coarser resolution based on a specified technique (Sum, Min, Max, Mean, or Median). Conceptually, the aggregate function works as follows:

- It multiplies the cell resolution of the input raster by the factor specified in the techniques. The resulting value correspond to the cell resolution of the output raster
- It maps the spatial extent of the output cells onto the input raster. Figure 6 shows an example of the output cell with thick line and input raster with thin line.
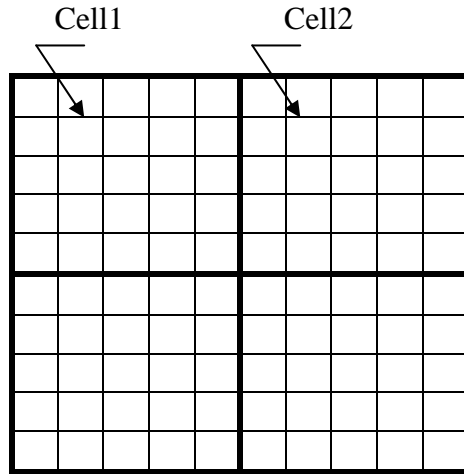
Figure 6 Output cell on top of input cell

- It identifies the cells on which to perform the aggregation calculations. Cell locations from the input raster that fall within the extent of an output cell are included in the calculations for determining that cell's output value
- It calculates the output value by determining the sum, minimum, maximum, mean, or median value of the cells from the input raster that fall within the output cell's spatial extent

The aggregation process was performed for the reclassified seven classes and was based on pixels aggregation from 25 to 250m. This process is expressed in a simple mathematical way as can see below:

$$Conversion-efficiency_{250m} = \frac{1}{N_p}\sum_{i=1}^{n} A_i * (\varepsilon)_i \qquad (25)$$

Where *A* is total number of pixels per land use type based on output scale, ε is the final light use efficiency (results of $\varepsilon_{g\text{-max}}$, ST_{min} and S_{VPD}) per land use type, N_p is the total number of pixel contained in the output scale (250m) and *n* is the number of classified land use type.

3.5.2 Derived NDVI from Surface reflectance

Before ordering the surface reflectance data MOD09, assessment of image quality was performed using MODIS Global browse images. The MODIS global browse images system was developed by the MODIS Land Science Team as coarse 5km versions of selected products to enable synoptic quality assessment on the internet prior to ordering the data. The site is located at http://landqa2.nascom.nasa.gov/cgi-bin/browse/browse.cgi. This site is useful to detect whether the image of a particular day is cloud or free from cloud. After assessing the quality of the image, sixty one images were ordered for the entire period of 2007. The surface reflectance image is in a new map projection called the Integerized Sinusoidal (ISIN)

projection. This product is supplied in hdf data format. The product contains several bands such as QC_250m_1, obscov_1, sur_refl_b01_1, sur_refl_b02_1, and num_observations. But for deriving NDVI only two bands are needed sur_ref_b01_1 and sur_ref_b02_1 the rest is not used.

The MODIS Reprojection Tool (MRT) was used to clip, georeference the image to the known projection system and split the bands of the modis data. The results were projected to UTM and stored in tiff format. NDVI was then derived using equation 9. ERDAS IMAGINE software was used to implemented the equation for NDVI calculation (equation 9). Figure 7 below indicate days over a year for which surface reflectance images were selected with less or no clouds. Zero represents day where no image is selected while one represents day where image is selected. In total sixty one surface reflectance images were ordered and used in this research.
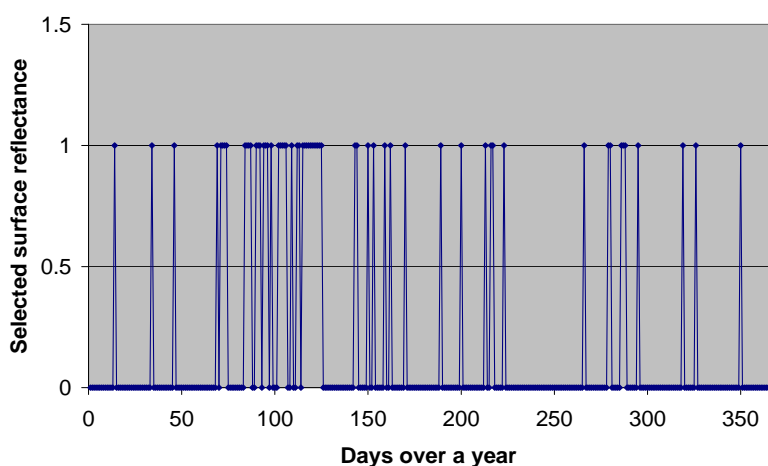
Figure 7 Available MODIS surface reflectance images (selected = 1) over the year 2007 for the Gendt area

3.5.3 Derive Light Use Efficiency

The light use efficiency ε was calculated from $\varepsilon_{g\text{-}max}$ (the biome-specific maximum conversion efficiency), which is reduced by the temperature modifier when low temperatures limit plant function, and a vapor pressure deficit (VPD) modifier, which reduces the maximum conversion efficiency when VPD is sufficiently higher enough to inhibit photosynthesis. The maximum light use efficiency value was extracted from different literature sources. The values of $\varepsilon_{g\text{-}max}$ per land use type were investigated as reported from different literature sources and it was found that for the same vegetation type these values vary from place to place. Therefore, two assumptions were applied in the selection of final $\varepsilon_{g\text{-}max}$ in this thesis. The value was chosen based on the location/country where the climate is comparable with Netherlands and in case of variation the average was used to get the final value. Table 5 below indicates the extracted values of maximum light use efficiency per land use type as compiled by Ahl et al. (2005) and Running et al. (2000).

Table 5 Maximum light use efficiency

Land use type (LU)	Maximum light use efficiency($\varepsilon_{g\text{-}max}$)	source
Grassland	0.3	Ahl et al., 2005
Cropland	3.0	Ahl et al., 2005
Mixed forest	0.42	Ahl et al., 2005
Deciduous broadleaf forest	0.53	Ahl et al., 2005
Open wetland/open shrubland	0.27	Ahl et al., 2005
Natural herbaceous vegetation	1.4	Running et al., 2000

The light use efficiency (ε) per land use type was derived based on scalar minimum temperature, scalar vapour pressure deficit and maximum light use efficiency as expressed below.

$$\varepsilon = (\varepsilon_{g-max} * ST_{min} * S_{VPD})$$ (26)

This equation was implemented in excel and the results are shown in appendix 2. These results were used as an input in (equation 25) the aggregation of LGN4 from 25m to 250m scale to obtain the final conversion efficiency.

3.5.4 Calculation of Daily GPP time series

Daily Gross primary production was derived based on the LUE model as the product of daily PAR, NDVI (equivalent to fPAR) and final conversion efficiency (equation 1). The calculation for single day GPP was done in ArcMap while time series of GPP were computed using a python script see appendix 1. The python script is very useful in GPP calculation since it helps to generate multiple results at once.

3.5.5 Calculation of Autotrophic respiration

The calculation for autotrophic respiration was separated in growth respiration (R_g) and maintenance respiration (R_a) components. Different literature sources (Heinsch et al., 2003, Running et al., 2000) have described the estimation of autotrophic respiration as the sum of maintenance respiration, R_m, from the three live vegetation components (leaves, stem, and root) and growth respiration, R_g. However, this thesis did not take into account vegetation components. A simple approach used by (Tao et al., 2005) was adopted in this thesis for estimation both growth and maintenance respiration. The autotrophic growth respiration was expressed as a proportion of GPP and assumed to be constant at 0.25. The estimation of growth respiration as 25% of GPP was implemented using the programmed python script and the results were generated to all available datasets (see appendix 3). The maintenance respiration algorithm used by Tao et al., (2005) requires above ground biomass of the vegetation. The biomass is derived based on minimum visible reflectance. Many authors have demonstrated that visible reflectance is positively related to standing biomass and canopy closure (Prince and Goward, 1995). Above-ground biomass was estimated based on the following expression;

$$W = 7166.1(\rho_{min}^{-2.6})$$ (27)

Where W is the above-ground standing biomass (Mg m^{-2}), and ρ is the minimum reflectance (ρ_{min}, %) in AVHRR channel 1. The AVHRR channel 1 is ranging between 0.57 – 0.71 μm, however, this was not used to calculate biomass in this thesis. The MODIS surface reflectance band 1 range between 0.62 – 0.67 was used in the estimation of biomass. This band was used because its range is similar to AVHRR channel 1. The surface reflectance band 1 product was multiplied with scale factor of 0.0001 as provided in a product description and the results were then reduced to percentage to obtain the final minimum surface reflectance (ρ_{min}, %). The calculation for the biomass (W) was performed in ERDA IMAGINE. Therefore, maintenance respiration was estimated based on the approach used by Tao et al., (2005).

$$R_m = 0.53 * (\frac{W}{W+50}) * e^{0.5}(\frac{Tc-T}{25})$$
(28)

Where *Tc* is the base temperature and is assumed to be constant at 25ºC, and *T* is the daily average temperature. The calculation for maintenance respiration is implemented in ERDA IMAGINE. Autotrophic respiration is then estimated as the sum of growth and maintenance respiration. The calculation was performed using the programmed python script (see appendix 5 and 6) to have the results for the all available datasets.

3.5.6 Calculation of Daily NPP time series and annual NPP

Daily NPP was estimated as the difference between daily GPP and autotrophic respiration. The calculation for daily NPP time series was implemented using python script (see appendix 7and 8) at a scale of 250m. Annual NPP was estimated as the sum of all the derived daily NPP over the year 2007. This calculation was implemented using ArcMap.

3.6   Comparison

Several methods can be used for comparison purposes, among them are maps comparison, point to point comparison or pixel to pixel comparison, and also comparison based on a particular land use type (Pan et al., 2006). This thesis was intended to do a comparison based on eight days GPP MODIS products (MOD17A2) with the derived daily GPP for the year 2007. Similarly, annual NPP MODIS product (MOD17A3) aimed for comparison with the derived annual NPP. However, due to the limitation in the availability of MODIS data for the year 2007, comparison was done based on the MODIS products of 2006. Because of the transformation of MODIS product from collection 4 to collection 5, MOD17A2/3 for the year 2007 was not available during research period until summer 2008. Therefore, the product of 2006 was used as an alternative for the comparison purposes. Two methods of comparison were adopted in this thesis: 1) map to map comparison and 2) pixel to pixel comparison based on temporal variability over a year.

Map to map comparison was done based on the results (maps) of time series of the derived daily GPP over the year 20007 with MOD17A2 2006. The map of the derived annual NPP 2007 was also compared to the map of the annual MODIS product (MOD17A2) 2006.

Pixel comparison was done only to the derived daily GPP 2007 and the MOD17A2 2006. Land use class per pixel was identified to the whole map by overlay with the reclassified LGN4. Pixel representing a single land use class was selected on the map and creating the time series of change in GPP over the year. Then pixel to pixel comparison was done based on the time series of the same selected land use class.

4 RESULTS

4.1 Photosynthetic active radiation

Figure 8 shows the time series of incoming photosynthetic active radiation (↓PAR) over the year 2007. The graph of ↓PAR follows the general incoming solar radiation pattern with spikes. The pattern appeared to be raised with short temporal range fashion from DOY1 until DOY126 (May 6) then started to have inconsistency variation with short and high temporal range until DOY221 (August 9) and started again having short temporal range fashion until DOY 365. The incoming PAR for the year 2007 appeared to be at maximum in DOY170 which is June 19. In general the entire pattern illustrates the seasonal changes in ↓PAR over a year 2007.
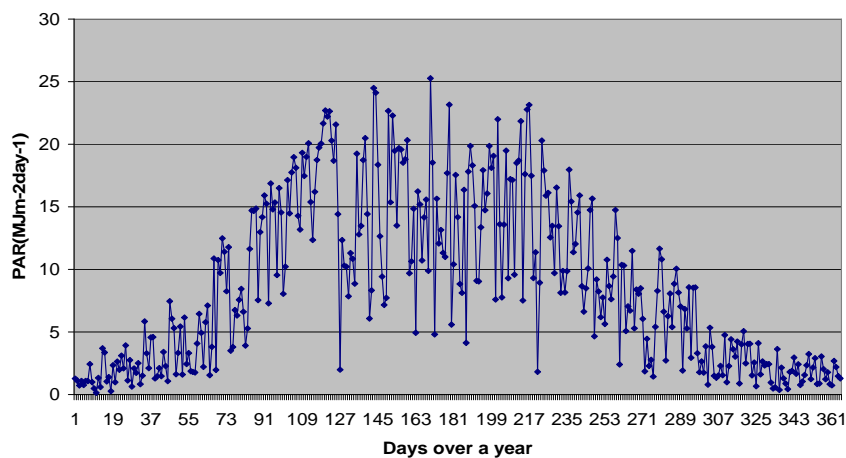
Figure 8 PAR time series over the year 2007 at Haarweg weather station

4.2 Vapor pressure deficit

Figure 9 shows the graph of vapor pressure deficit time series for the year 2007. The pattern of figure 9 shows a similar pattern to solar energy with short temporal range in winter seasons and both short and high temporal range during the summer. An interesting part in this figure is the sudden rise in VPD at the start of DOY85 until DOY90 and DOY102 till DOY124. After DOY124 the VPD suddenly fall and became lower with short temporal range until DOY365.
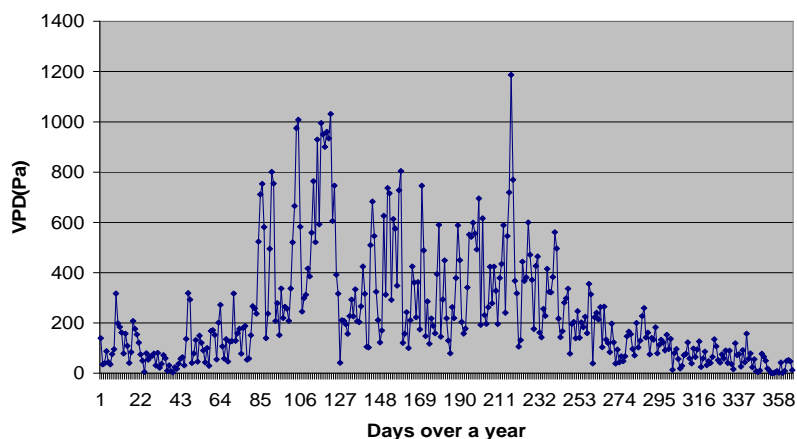
Figure 9 VPD time series 2007 at WUR weather station

26

4.3 GPP variability based on LUE approach

Figure 10 shows the results of time series daily GPP 2007 for grass, crop and deciduous forest. The time series of daily GPP per land use class is based on one pixel per land use type. Grass, crop and deciduous forest seems to follow a similar pattern at different seasons over a year. However, the magnitude of GPP for grass and crop are much related in the entire seasons while for deciduous forest is much closer with grassland and cropland in winter season and differs in summer period. Figure 10 indicates lower GPP in winter season and high GPP in summer. The maximum value of GPP for grass is 18 gC m^{-2}, crop is 20 gC m^{-2}, and deciduous forest is 8 gC m^{-2}. In summer there is a sudden drop of GPP at DOY162, DOY200 and DOY213 for all three vegetation types.

Figure 11 shows the time series of NDVI for grass, crop and deciduous forest in 2007. The pattern of all three vegetation types is similar for the entire period of 2007. The highest peak of NDVI for all vegetation types is the same (0.8). DOY100, 162 and 200 shows the sudden fall of NDVI with respect to regular pattern of the season.

Figure 12 shows the time series of light use efficiency for grassland, deciduous forest and cropland in 2007. The light use efficiency for deciduous forest shows to be much lower compared to grassland and cropland.
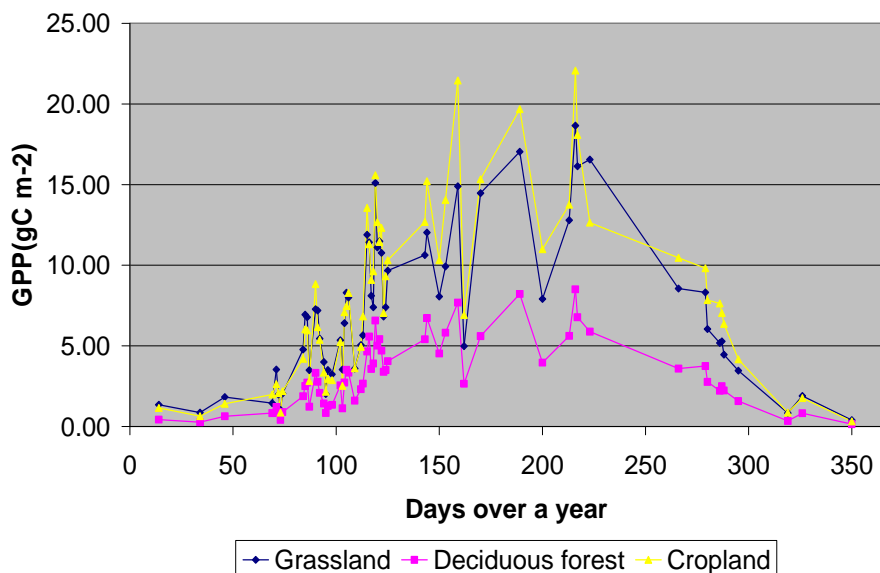
Figure 10 Daily GPP for grass, crop and deciduous forest 2007
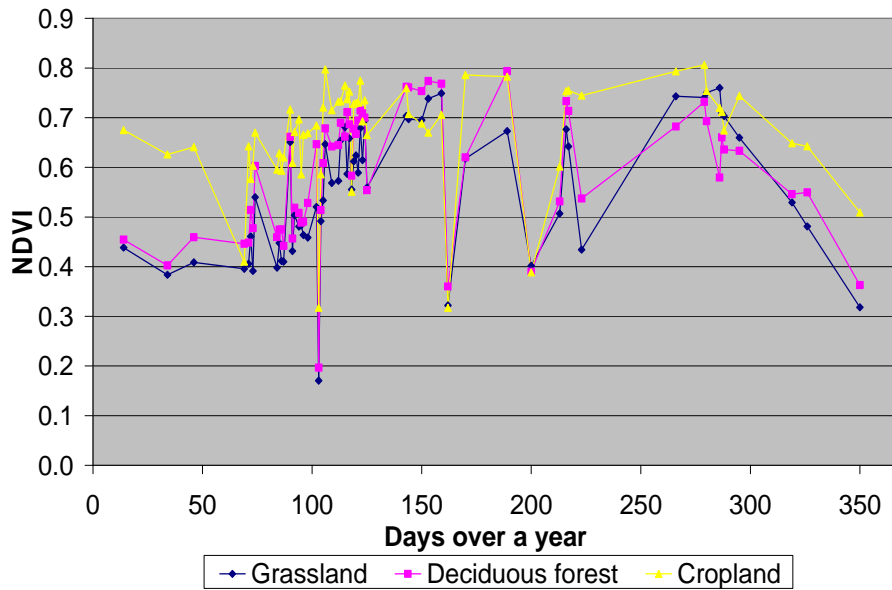
Figure 11 NDVI for Grassland, cropland and deciduous forest 2007
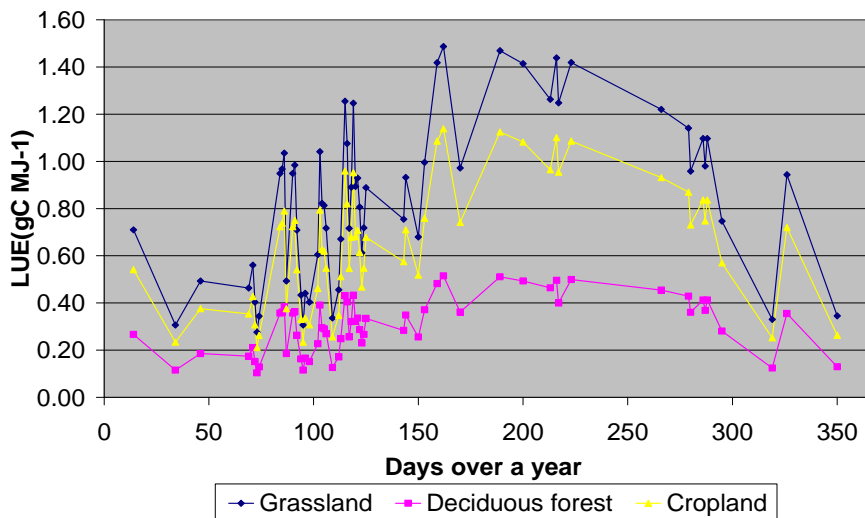
Figure 12 Light use efficiency for Grassland, Deciduous forest and Cropland

4.4   NPP variability based on LUE approach

Figure 13 shows the result of time series daily NPP for grassland, cropland and deciduous forest over the year 2007. The time series of daily NPP per land use class is based on one pixel per land use type. The pattern of the graph follows the sinusoidal pattern of PAR over the year. The estimated daily NPP became lower than the estimated daily GPP. The maximum values of NPP for grass and crop are 14 gC m^{-2} and for deciduous forest is 6gC m^{-2}. Figures 14, 15, and 16 indicate the comparison of net primary production and autotrophic respiration for crop, deciduous forest and grass respectively. Figure 15 indicates few days with NPP below zero for deciduous forest in winter season. Figure 17 shows the results of the derived annual NPP 2007 range between 44 and 391gC m^{-2}.

28
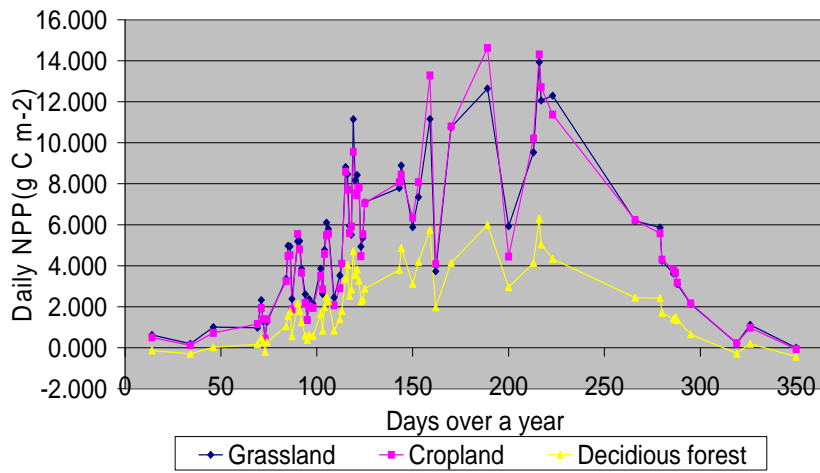
Figure 13 Derived daily NPP for grassland, cropland and deciduous forest 2007
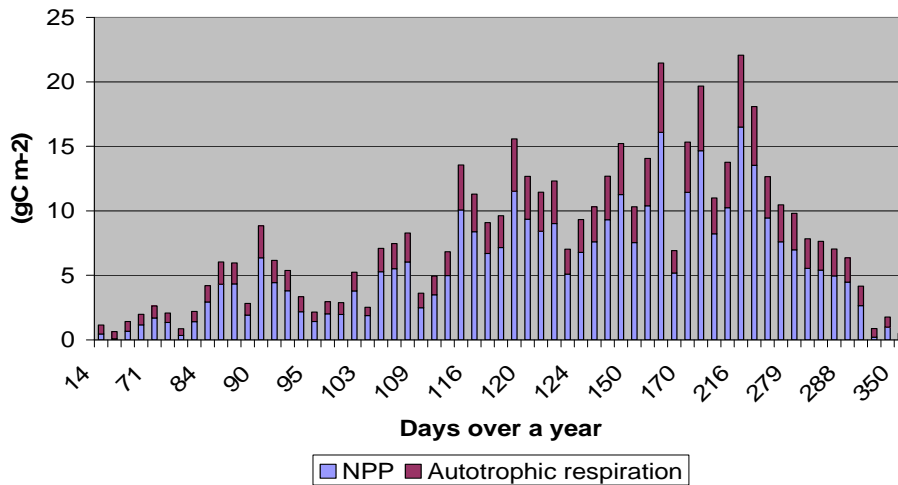
Figure 14 Net primary production and autotrophic respiration for crop
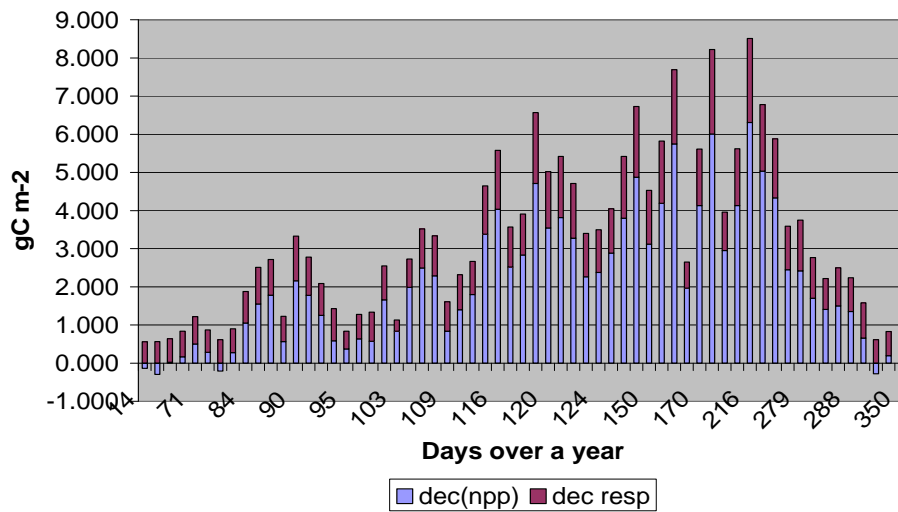
Figure 15 Net primary production and autotrophic respiration for deciduous forest
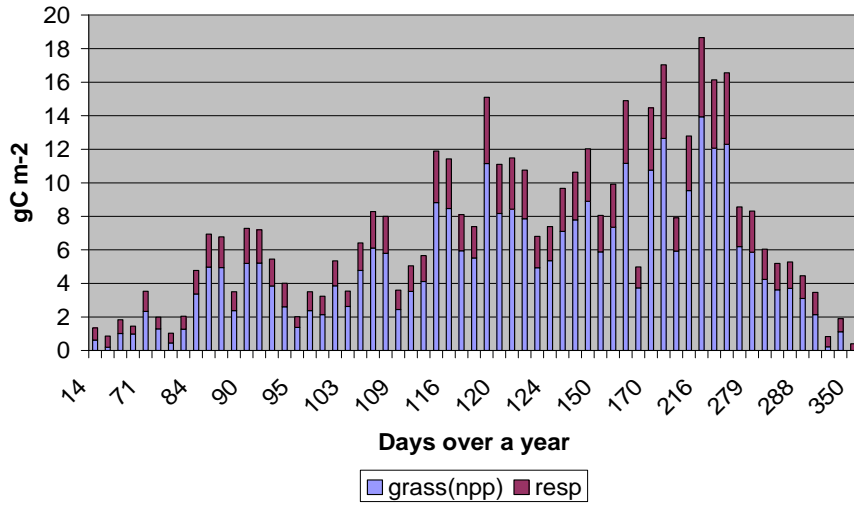
Figure 16 Net primary production and autotrophic respiration for grass
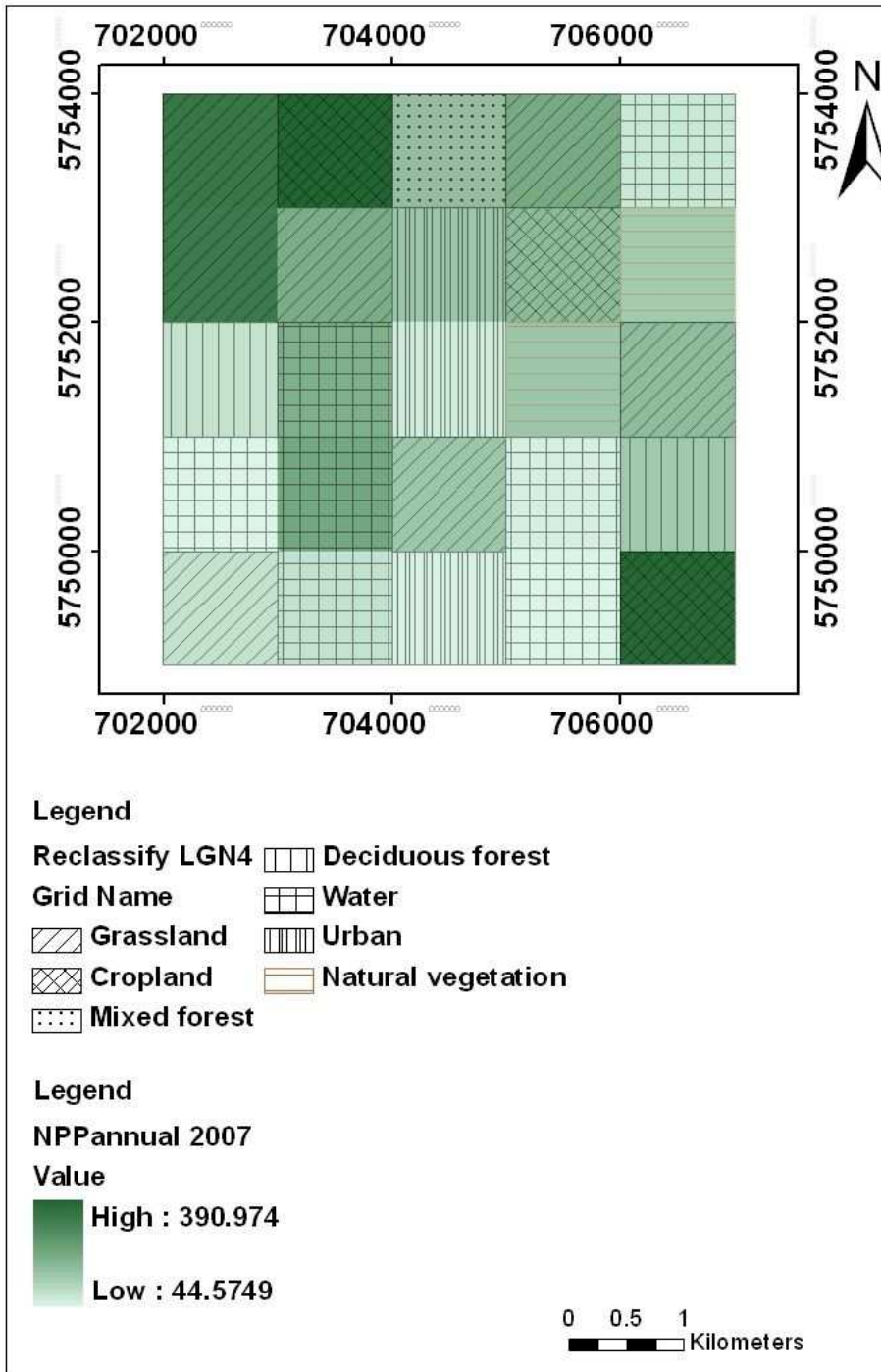
Figure 17 A derived map of annual NPP 2007

4.5 Comparison of MODIS product 8-days GPP 2006 and derived daily GPP 2007

4.5.1 Map to Map comparison

Figure 18 shows the graph of correlation between time series of MODIS product 8 days GPP 2006 (MOD17A2) against the derived daily GPP 2007. Each point on the figure represents GPP (gC m^{-2}) and the equation indicates linear correlation between MODIS product GPP and the derived GPP. The linear correlation between the two products indicates the slope of 0.72

with R^2 of 0.11. The values for MOD17A2 range from 0 – 63 gC m^{-2} while the derived GPP range from 0 – 23 gC m^{-2}.

Figure 19 shows the result of GPP map derived by subtracting MOD17A2 2006 and the derived GPP 2007. These maps were selected for single day (June 2) which appeared to have the highest values of GPP for MOD17A2. The result of the GPP map between MOD17A2 and derived GPP indicates the range from 7 – 58 gC m^{-2}. White pixels in figure 19 were regarded as no data after discovered that their GPP values for MOD17A2 are greater than 30000.
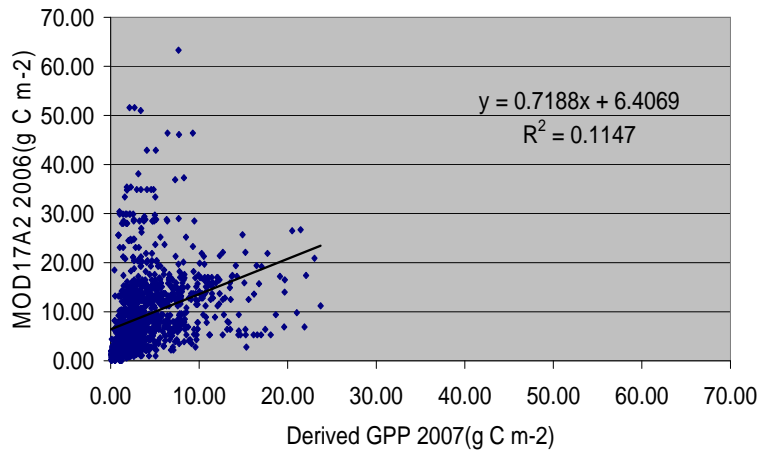
Figure 18 MOD 17A2 2006 and derived GPP 2007
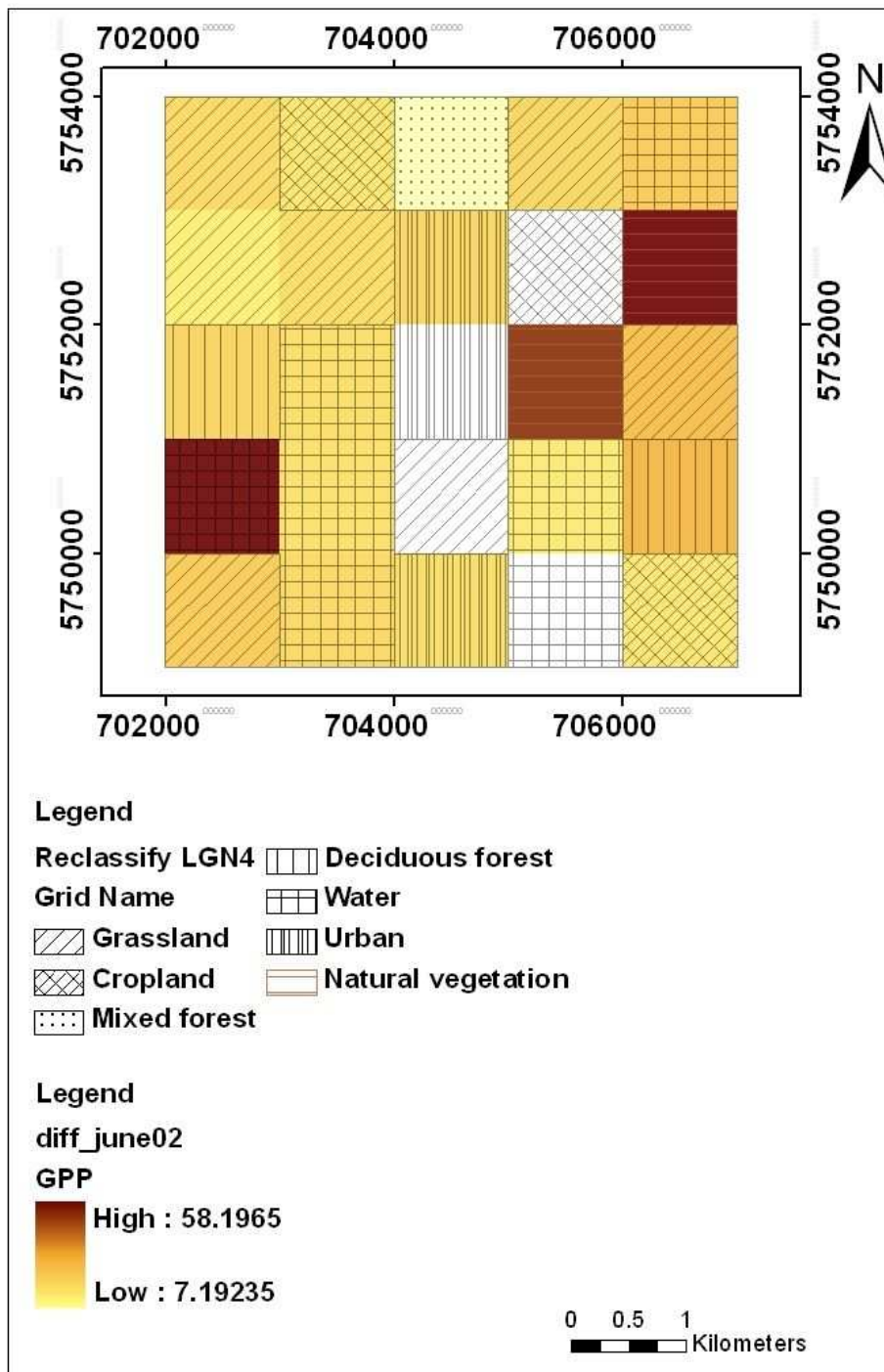
Figure 19 Map of difference between MOD17A2 2006 and derived GPP 2007

4.5.2 Comparison of individual land cover classes

Figure 20 shows the time series of MODIS product 8 days GPP 2006 (MOD17A2) and derived daily GPP 2007 for grassland based on a single pixel. The pattern for the two products has much similarity in temporal variation and differs in the maximum range of GPP. Figure 21 shows the correlation graph based on the comparison of MOD17A2 2006 and derived daily GPP 2007 for grassland. Each point on the graph indicates the magnitude of GPP and the equation also indicate slope of 0.81 with R^2 of 0.406.

Figure 22 shows the time series of MODIS product and derived daily GPP for cropland also based on single pixel. The pattern for the two products seems to be similar for the entire

season but differs slightly in maximum range. Figure 23 shows the correlation graph based on comparison of MODIS product (MOD17A2) and derived daily GPP for cropland. Each point on the graph indicates the amount of GPP and the equation also indicate slope of 0.77 with R^2 of 0.5055.

Figure 24 shows the time series of MODIS product and derived daily GPP for deciduous forest based on single pixel. The graphs for deciduous forest indicate similar pattern but differs in the scale of GPP. Figure 25 shows the correlation graph of MODIS product (MOD17A2) 2006 and derived daily GPP 2007 for deciduous forest. Each point on the graph indicates the scale of GPP and the equation also indicate slope of 2.30 with R^2 of 0.522.
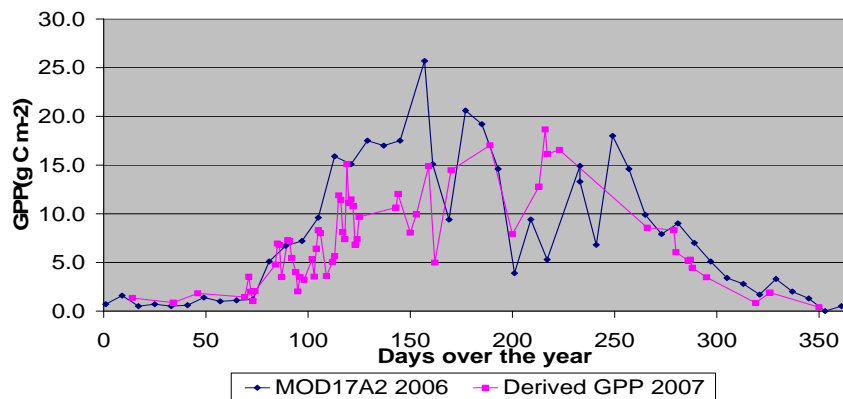
Figure 20 Comparison of MOD17A2 2006 and Derived GPP 2007 for grassland
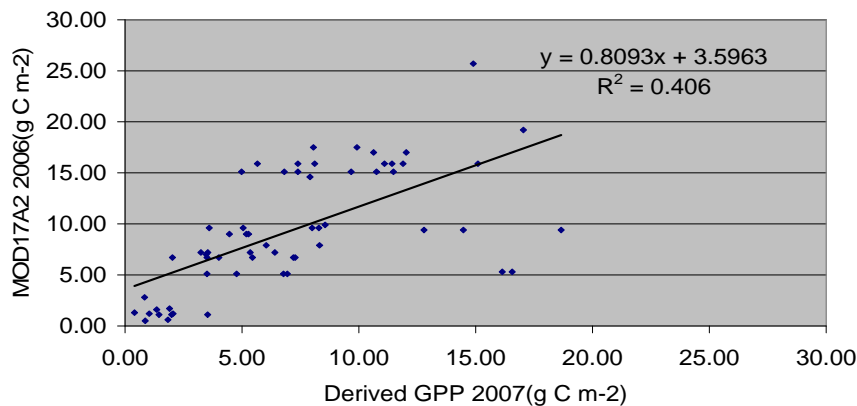
Figure 21 Pixel correlation for grassland between MOD17A2 2006 and derived GPP 2007
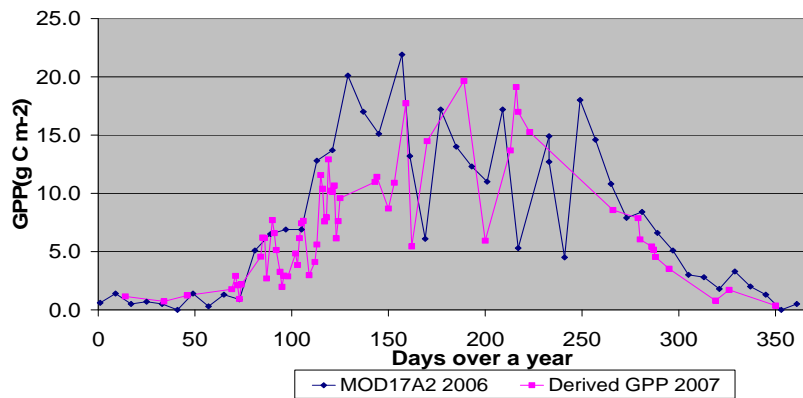
Figure 22 Comparison of MOD17A2 2006 and Derived GPP 2007 for Cropland

$$y = 0.7684x + 3.1963$$
$$R^2 = 0.5055$$
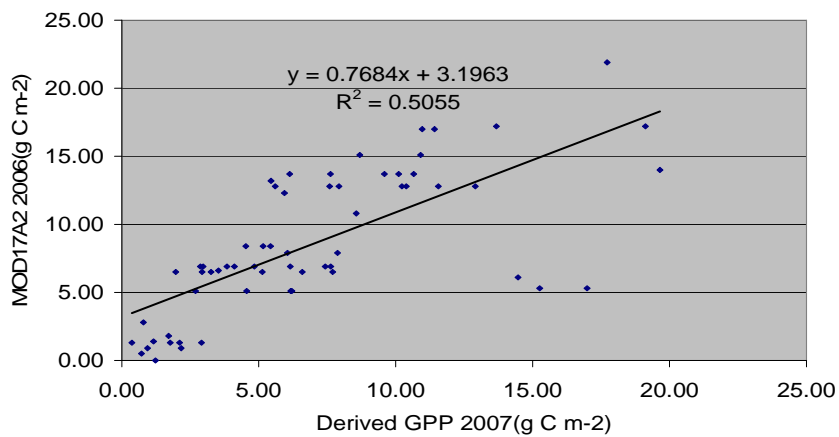
Figure 23 Pixel correlation for cropland between MOD17A2 and derived GPP
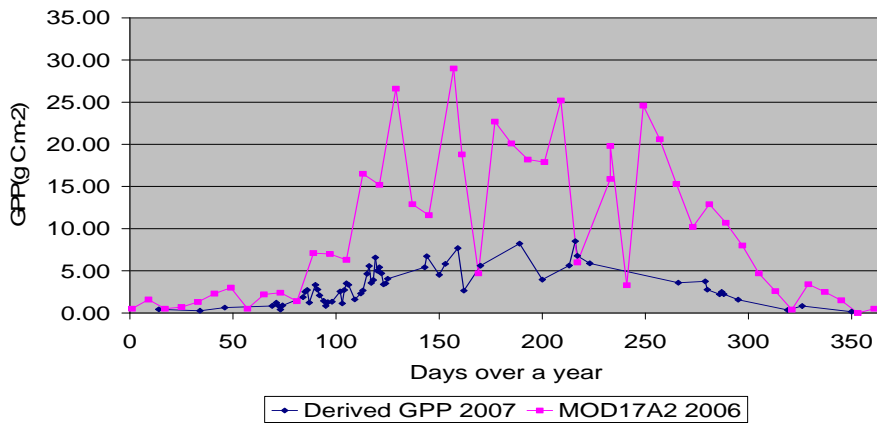
Figure 24 Comparison of MOD17A2 2006 and derived GPP 2007 for deciduous forest
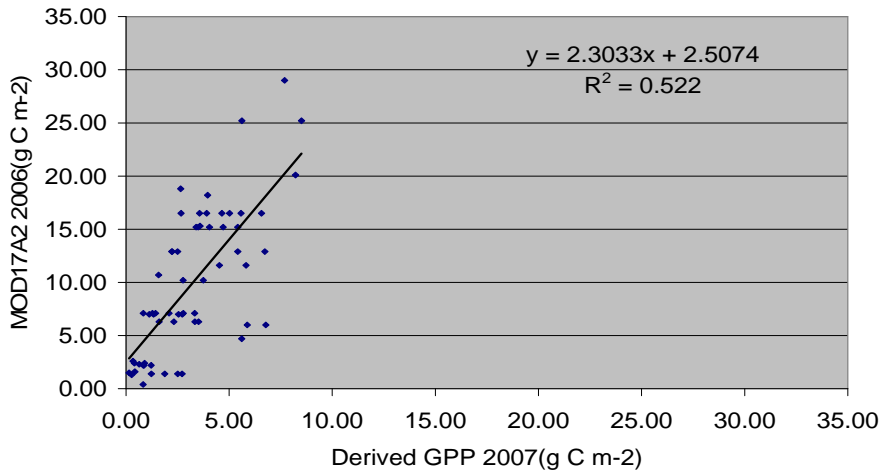
Figure 25 Pixel correlation for deciduous forest between MOD17A2 and derived GPP

4.6 Comparison of MODIS product annual NPP 2006 and derived annual NPP 2007

Figure 26 shows the graph of correlation between MODIS product annual NPP 2006 (MOD17A3) and the derived annual NPP 2007. Each point on this figure represents the values of annual NPP. The distributions of points on the graph are scattered horizontal and the equation indicates a slope of -0.06 with R^2 of 0.005.

Figure 27 shows the result of NPP map derived by subtracting MOD17A3 2006 and the derived annual NPP 2007. White pixels in this figure were regarded as no data after discovered that their NPP values for MOD17A2 are greater than 30000.
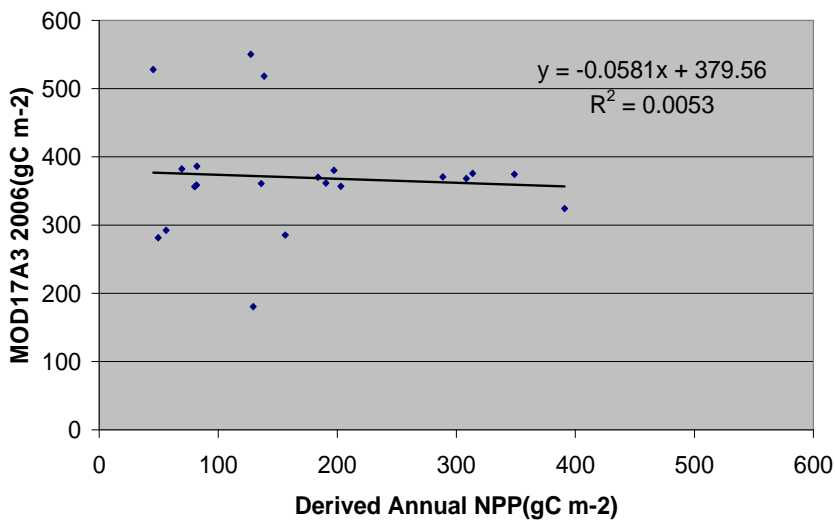

Figure 26 Correlation between MOD 17A3 2006 and derived annual NPP 2007
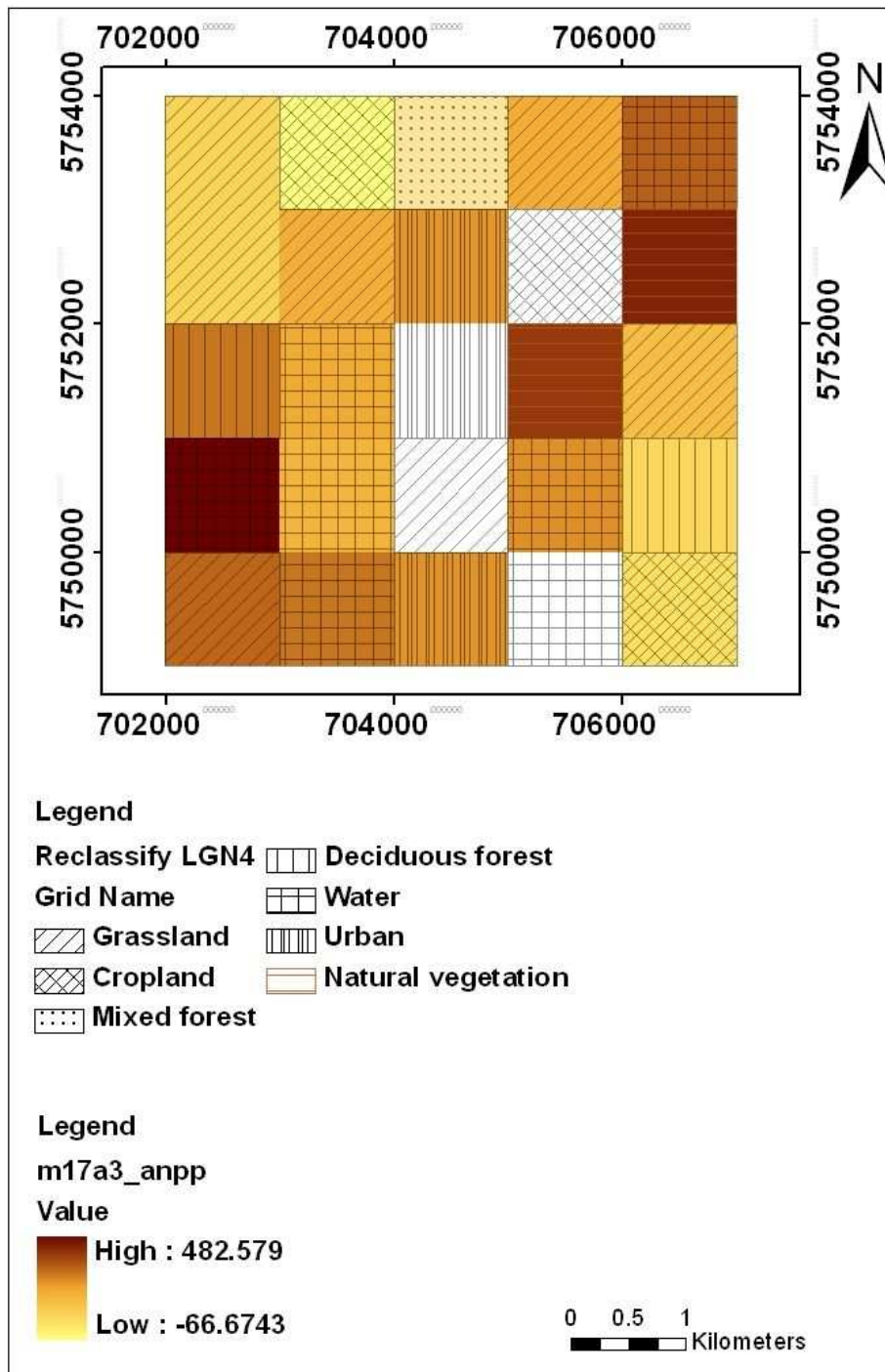
Figure 27 Map of difference between MOD17A3 2006 and derived annual NPP 2007

5 DISCUSSION

5.1 Photosynthetic active radiation

The pattern of figure 8 indicates seasonal changes in ↓PAR similar to general pattern of incoming solar radiation. The seasonal pattern of ↓PAR over a year is appeared due to the variations in the earth-sun distance cause small alterations in the solar constant, and the tilt of the earth's axis results in variations in day length as well as the angle of incidence, similar to latitudinal effects. The Netherlands are located towards northern hemisphere where intensity is reduced by the low sun angles of the winter and increased by the higher angles of the summer.

The short temporal range in the amount of ↓PAR as have seen on figure 8 varies with latitude and time of day. Within a day, the sun travels across the sky with a change in its altitude from sunrise to sunset. The intensity and spectrum of direct sunlight depend strongly on the path length of the beam and on the solar angle.

The short and high temporal range of ↓PAR as have seen in figure 8 from DOY126 (May 6) until DOY221 (August 9) is due to transmission conditions in the atmosphere (cloud cover, aerosols). Clouds are the largest modulators of the solar radiative flux reaching the Earth's surface. The amount and type of cloud cover prevailing at a given time and location largely determines the amount of solar radiation received at the Earth's surface. Although solar radiation is relatively constant at the top of the atmosphere, all of these processes combine to create large variations in the amounts of PAR and solar energy available at the surface of the earth. The effect of clouds is much bigger in summer (e.g. DOY126 – DOY221) since the amount of ↓PAR on the Earth surface is much higher in summer with clear sky.

5.2 Temperature and vapor pressure deficit

Figure 9 shows the pattern of VPD with short temporal range in winter season and both short and high temporal variation is summer. The measurements used to derive VPD were examined relative to winter and summer seasons. The investigation has revealed that the temperature and relative humidity measured in winter season have small variation. However, the change in weather such as free sky (cloudiness) can also determine the scale of temperature and relative humidity measured in winter season. In general relative humidity is usually high at midnight and in the early morning, drops rapidly, after the sun rises, until it is lowest just after midday depending on the climate/weather. Figure 9 shows the reality of how weather can determine the scale of VPD though the season is winter. It indicates the high value of VPD from DOY85 (March 26) until DOY90 (March 31) and DOY102 (April 12) till DOY124 (May 4). This period in Netherlands usually is winter season but in 2007 the climate was dry results in high values of VPD. Between DOY85 and DOY90 the average temperature was 11°C while average RH was 65% and DOY102 to DOY124 the average temperature was 16°C while average RH was 62%. Figure 10 also indicates relatively high temperatures for the same corresponding days.

The pattern of VPD over the year with both short and high temporal range is also caused by the variation in weather. However, the effect in summer is bigger due to high temperature and low relative humidity during a day.

5.3   GPP variability based on LUE approach

The pattern of figure 10 for daily GPP over the year 2007 is related with parameters used in its derivation. This pattern seems to be similar with sinusoidal pattern of PAR over the year. The increase in PAR is proportional to the increase in GPP for all vegetation types. Figure 10 also shows lower GPP of deciduous forest compared to grassland and cropland. The lower values of GPP for deciduous forest was caused by the low values of light use efficiency as indicated in figure 12. Cropland appeared to have high GPP than grassland though the light use efficiency for cropland is lower than grassland as can see figure 12. This effect was caused by the high values of NDVI for cropland compared to grassland however the difference between them is smaller as indicated in figure 11.

Figure 10 shows the suddenly fall of GPP at DOY125, DOY162, and DOY200 similar to figure 11 which also indicates the suddenly falls of NDVI for the same corresponding days. The sudden fall of GPP and NDVI was caused by the effect of cloudiness to surface reflectance on the vegetation cover. Cloud-contaminated measurements produce lower NDVI values, as clouds reflect strongly in both the red and near-infrared wave bands. The low values of NDVI caused the same effect to GPP since these two are linear related.

The validity of the derived GPP results based on selected land use classes were assessed by examines the reported values of GPP in different literature sources with similar land use type. This thesis did not perform any validation rather it just compared the range of the reported value of GPP. MODIS products are validated using the measured data from eddy covariance flux tower. Turner et al. (2005) has reported the range of GPP for cropland to be 0 and 13gC m^{-2} as measured by eddy covariance flux tower. The range of the derived GPP in this thesis for cropland is 0 and 20gC m-2 which comply with flux tower GPP. The range for deciduous forest from flux tower reported GPP of 0 and 12gC m^{-2} while the thesis derived GPP is 0 and 8gC m^{-2} which also shows similarity.

5.4   NPP variability based on LUE approach

The results of the derived daily NPP for grass, crop and deciduous forest are lower than the derived daily GPP. This is because of autotrophic respiration factor. Figure 13 shows the graph of time series daily net amount of primary production for different land use types after take out the maintenance and growth respiration. Figures 14, 15 and 16 indicate the rate of autotrophic respiration increases with respect to growth of plant. Higher values of NPP and R_a both appeared in summer season. Low values of NPP and R_a appeared in winter season because of stoppage of vegetation growth at this period. The NPP below zero for deciduous forest shown in figure 15 during winter season is an indicative to the effect of using similar parameters in derived autotrophic respiration to all land use type. For this study the effect appeared to deciduous forest only. This effect is due to estimation of biomass for deciduous forest. Figure 17 indicates higher annual NPP for cropland and grassland compared to other land use type such as deciduous forest. This is because of higher light use efficiency for both crop and grass compared to deciduous forest as can see figure 12. Lower annual NPP values are shown to water and urban area as expected.

5.5 Comparison of MODIS product 8 days GPP 2006 and derived daily GPP 2007

5.5.1 Map to Map comparison

Figure 18 shows that the correlation between the derived daily GPP and MOD17A2 is poor with R^2 equal to 0.11. This relation indicates that temporal variation of GPP over the year between 2006 for MOD17A2 and 2007 for derived GPP were inconsistency. However, the difference in range of temporal GPP between the two products is low as the slope close to one (0.71). Figure 19 spot specific pixel and the land use type with higher difference of GPP between the two products. Three pixels with land use type were identified to have higher difference in GPP. The land use type belong to these pixels are water and natural vegetation. Considering components used in derived GPP algorithm, the higher difference between the two products are due to 1) maximum light use efficiency were used to generate GPP at the identified pixels was different. The maximum light use efficiency used to derive GPP in this thesis was based on LGN4 (25m resolution) which signifies heterogeneity landscape while for MOD17A2 product is derived based on land cover MODIS product (MOD12Q2) at 1km resolution. 2) Change in management of land use to the pixels identified as natural vegetation is the source of higher difference. This is because the comparison of the two products was based on different years 2006 and 2007.

Turner et al. (2005), reported that MODIS products are underestimated GPP for crop because of the low value of ε_{g-max} used from the biome properties lookup table. He pointed out that the value of ε_{g-max} used by MODIS for crop is 0.68gC MJ^{-1} while based on tower flux measurements is on the order of 3gC MJ^{-1}. After examine the ε_{g-max} used in MODIS product for different land use classes it is clear that this thesis has used different ε_{g-max}. Heinsch et al. (2003) has reported the ε_{g-max} used in MODIS product as 0.68gC MJ^{-1} for crop, 1.01 gC MJ^{-1} for deciduous forest, 0.68 gC MJ^{-1} for grass, 0.77 gC MJ^{-1} for open shrub and 1.11 for mixed forest. None of the reported ε_{g-max} used by MODIS complies with ε_{g-max} used in this study. The ε_{g-max} of 3gC MJ^{-1} for crop based on flux tower complies with the research ε_{g-max} used to derive GPP for crop.

5.5.2 Comparison of individual land cover classes

The results of the comparison between MOD17A2 2006 and the derived daily GPP 2007 for grassland, cropland, and deciduous forest indicate a good correlation with R^2 of 0.406, 0.505, and 0.52 respectively. Figures 20, 22, and 24 have shown similar pattern for both MODIS product and derived GPP for the entire seasons. The comparison of difference in values of temporal GPP for crop and grass is very small with slope close to 1. Grass shows the slope of 0.81, and crop shows the slope of 0.77. For deciduous forest the comparison shows much deference in the values of GPP. Figure 25 shows the slope of 2.30 which gives an indication that the derived GPP is lower than MODIS to the factor of 2.30. This difference is caused by lower ε_{g-max} for deciduous forest used in this study (0.53gC MJ^{-1}) compared to higher ε_{g-max} used in derived MODIS GPP (1.04gC MJ^{-1}).

5.6 Comparison of MODIS product annual NPP 2006 and derived annual NPP 2007

The result of figure 26 shows no correlation on the comparison of annual NPP MODIS product (MOD17A3) 2006 and the derived annual NPP 2007 with R^2 of 0.005. This is an expected result because in the comparison of daily GPP no correlation was found between the two products. The sources of uncorrelated in annual NPP for MODIS product and derived NPP is similar as happened for GPP. These sources were described in detailed in section 5.5.1 map to map comparison. However, this research is also considered autotrophic respiration as another source because different approach was used to derived growth and maintenance respiration.

Figure 27 was used as an indicative to identify land use type with higher values appeared in figure 26 for MOD17A3. The land use classes with higher values of NPP were identified as water and natural vegetation. In reality pixel with water is not supposed to have higher NPP than other land use type. That means MODIS product was used different maximum light use efficiency to derive GPP to pixel belong to water. For natural vegetation both maximum light use efficiency and management of land use parcel are the sources of this difference.

Figure 27 shows white pixels which were regarded as no data because in the MOD17A3 product four pixels were found to have value >30000. According to Heinsch et al (2003), pixel with value greater than 3000 is referred to as non-modelled, thus should not used in the analysis.

6 CONCLUSIONS AND RECOMMENDATIONS

6.1   Conclusions

The objective of this research was to demonstrate a method for integrating remote sensing and sensor web data for estimation of NPP at the Gendt location. The research reviewed different approaches for NPP estimation, i.e. LUE, CASA, GLO-PEM, TURC, and SDBM. The strategies for each model were identified and compared with respect to research objective and the light use efficiency (LUE) model was found to satisfy the criteria used to evaluate the appropriate model for the research. Therefore, this approach was adopted in this thesis.

Literature review has revealed different possibilities of parameterized light use efficiency model. In depth study was done for each model parameters including their limitation in terms of data availability and appropriate method was selected for parameterization.

Modeling implementation in this research was involved different data sources with varied spatial and temporal scaling. Scaling compatibility both spatial and temporal was inevitable during model implementation. Aggregation and resampling techniques was used in harmonizing spatial scaling while integration and average techniques was used to harmonize temporal scaling. Both techniques have proved to work properly in this research on both spatial and temporal scaling.

The results obtained from the derived daily GPP 2007 shows no consistency with MODIS product 8 days GPP 2006 (MOD17A2) for the entire map. However, similarities were found on land use class identified at some locations in the study area. Grassland and cropland has proved to be more consisted while other land use types show inconsistency such as natural vegetation, mixed forest and deciduous forest. The difference in result between MOD17A2 2006 and derived daily GPP 2007 were identified as; 1) the use of different maximum light use efficiency in the estimation of GPP, 2) change in management of land use parcel at some locations within the study area and 3) comparison was done based on products of different years.
The results obtained from the derived annual NPP 2007 shows inconsistency with MODIS product annual NPP 2006. Sources of their difference were identified to be the same as for GPP. The parameters used for estimation growth and maintenance respiration were different for each product and was considered as the source of their difference in NPP estimation.

The literature review has revealed three different ways of comparison the result obtained from the derived daily GPP and MODIS product. These methods are map to map comparison, pixel to pixel comparison and the comparison based on land use type. The first two methods were adapted in this thesis based on temporal variation over a year and has proved to be very useful for comparison purpose. This thesis did not perform any validation but possibilities to validate the results are to compare with data collected in eddy covariance flux tower and to compare with annual yield collected by farmer or institution. The validation process based on data from flux tower need to be setup in advance since it has some limitations. These limitations are 1) the validation data sets should be wall-to-wall surfaces 2) The spatial and temporal resolution of the validation products should closely match those of the derived products and 3) The components of the derived NPP/GPP algorithm should be analyzed along with the products themselves so as to interpret possible errors or limitations.

This research has produced different kind of results which were enough to be examined the possibility of applied the GPP/NPP approach elsewhere. The study has revealed that using coarse scale data at local level results in underestimation or overestimation of GPP/NPP. The effect of underestimation and overestimation differs in spatial and temporal scale. Spatially, the study has revealed that coarse scale data misleading the perfect location to apply maximum light use efficiency to derived GPP. This research has revealed that the pixel with high annual NPP for MODIS product was covered by water. Therefore, generalization performed to coarse spatial information increases uncertainty when applied in local level. In temporal scale, the study has revealed that the result of the daily change in GPP was direct related to environmental change. The amount of GPP for every single day in this thesis was changed according to the change in weather condition. Therefore, real time information provides a better estimation of current status of GPP.

The uncertainty detected in this thesis based on the results obtained is the application of autotrophic respiration parameters to all land use type. The results of NPP for deciduous forest in winter season was indicate values below zero. Though the values were found to be small but it was against the expectation.

The results of the derived daily GPP in 2007 have shown similarity in range with the results based on flux tower for cropland and deciduous forest. The approach used to generate the results for GPP indicates success in this thesis. This is because the method was used large scale spatial information and high temporal scale information. No limitations were found for implementation of each parameter used to derive GPP. Therefore, the method can be used anywhere at local level if sensor information and large scale remote sensing data is available.

6.2   Recommendations

This research has shown that the demonstrated methods for GPP/NPP estimation based on remote sensing and sensor web data at local scale level is feasible. Nevertheless, the demonstrated method was the first step to assess its applicability and efficiency at local scale level. Some recommendations are:

1. Further research need to be undertaken on NPP estimation to understand the effect of algorithm used for maintenance and growth respiration as applied to all vegetation type.
2. It would be of much interest in future if the result obtained from similar approach being validated using data from eddy covariance flux tower.

The demonstrated method in this thesis can be useful in future to avoid the problem of underestimate and overestimate GPP/NPP at local scale level.

Reference

ABDI, T., BULSINK, D. J., VAN DER BURGT, L., DALSTRA, H., GUAN, X., JUNWEI, Z. & KALAIAH, S. V. (2007) 'Presenting sensor data real-time in google earth': Sensors as a data sources for the SDI. *AMCII report.* Wageningen University.

AHL, D. E., GOWER, S. T., MACKAY, D. S., BURROWS, S. N., NORMAN, J. M. & DIAK, G. R. (2004) Heterogeneity of light use efficiency in a northern Wisconsin forest: Implications for modeling net primary production with remote sensing. *Remote Sensing of Environment,* 93**,** 168-178.

AHL, D. E., GOWER, S. T., MACKAY, D. S., BURROWS, S. N., NORMAN, J. M. & DIAK, G. R. (2005) The effects of aggregated land cover data on estimating NPP in northern Wisconsin. *Remote Sensing of Environment,* 97**,** 1-14.

CANADELL, J. G., MOONEY, H. A., BALDOCCHI, D. D., BERRY, J. A., EHLERINGER, J. R., FIELD, C. B., GOWER, S. T., HOLLINGER, D. Y., HUNT, J. E., JACKSON, R. B., RUNNING, S. W., SHAVER, G. R., STEFFEN, W., TRUMBORE, S. E., VALENTINI, R. & BOND, B. Y. (2000) Carbon metabolism of the terrestrial biosphere: A multitechnique approach for improved understanding. *Ecosystems,* 3**,** 115-130.

CAO, M., PRINCE, S. D., SMALL, J. & GOETZ, S. J. (2004) Remotely sensed interannual variations and trends in terrestrial net primary productivity 1981-2000. *Ecosystems,* 7**,** 233-242.

CHIEN, S., CICHY, B., DAVIES, A., TRAN, D., RABIDEAU, G., CASTAN?O, R., SHERWOOD, R., MANDL, D., FRYE, S., SHULMAN, S., JONES, J. & GROSVENOR, S. (2005) An autonomous earth-observing sensorweb. *IEEE Intelligent Systems,* 20**,** 16-24.

CHURKINA, G. & RUNNING, S. W. (1998) Contrasting climatic controls on the estimated productivity of global terrestrial biomes. *Ecosystems,* 1**,** 206-215.

CRAMER, W., KICKLIGHTER, D. W., BONDEAU, A., MOORE, B., III, CHURKINA, G., NEMRY, B., RUIMY, A., SCHLOSS, A. L. & "POTSDAM'95", P. O. (1999a) Comparing global models of terrestrial net primary productivity (NPP): Overview and key results. *Global Change Biology 5 (Suppl.1):1-15.*
.

CRAMER, W., KICKLIGHTER, D. W., BONDEAU, A., MOORE III, B., CHURKINA, G., NEMRY, B., RUIMY, A. & SCHLOSS, A. L. (1999b) Comparing global models of terrestrial net primary productivity (NPP): Overview and key results. *Global Change Biology,* 5**,** 1-15.

DAUGHTRY, C. S. T., GALLO, K. P., GOWARD, S. N., PRINCE, S. D. & KUSTAS, W. P. (1992) Spectral estimates of absorbed radiation and phytomass production in corn and soybean canopies. *Remote Sensing of Environment,* 39**,** 141-152.

FIELD, C. B., RANDERSON, J. T. & MALMSTROM, C. M. (1995) Global net primary production: Combining ecology and remote sensing. *Remote Sensing of Environment,* 51**,** 74-88.

GAMON, J. A., PENUELAS, J. & FIELD, C. B. (1992) A narrow-waveband spectral index that tracks diurnal changes in photosynthetic efficiency. *Remote Sensing of Environment,* 41**,** 35-44.

GAMON, J. A., SERRANO, L. & SURFUS, J. S. (1997) The photochemical reflectance index: An optical indicator of photosynthetic radiation use efficiency across species, functional types, and nutrient levels. *Oecologia,* 112**,** 492-501.

GOETZ, S. J., PRINCE, S. D., SMALL, J. & GLEASON, A. C. R. (2000) Interannual variability of global terrestrial primary production: Results of a model driven with

satellite observations. *Journal of Geophysical Research D: Atmospheres,* 105**,** 20077-20091.

GOETZ, S. J. & PRINCE, S. N. (1999) Modelling terrestrial carbon exchange and storage: Evidence and implications of functional convergence in light-use efficiency. *Advances in Ecological Research,* 28**,** 57– 92.

GOWER, S. T., KUCHARIK, C. J. & NORMAN, J. M. (1999) Direct and indirect estimation of leaf area index, f(APAR), and net primary production of terrestrial ecosystems. *Remote Sensing of Environment,* 70**,** 29-51.

GUILLAUME, G. D., KARL, F. H., FORREST, G. H., ELIZABETH, M. M., BLACK, T. A., ALAN, G. B., AND & HANK, A. M. (2005) A MODIS-derived photochemical reflectance index to detect inter-annual variations in the photosynthetic light-use efficiency of a boreal deciduous forest. *Remote Sensing of Environment,* 98 (2005) 212 – 224.

HAZARIKA, M. K., YASUOKA, Y., ITO, A. & DYE, D. (2005) Estimation of net primary productivity by integrating remote sensing data with an ecosystem model. *Remote Sensing of Environment,* 94**,** 298-310.

HAZEU, G. W. (2006) Land use mapping and monitoring in the netherlands(LGN5). *Proceedings of the 2nd Workshop of the EARSeL SIG on Land Use and Land Cover.*

HEINSCH, F. A., REEVES, M., VOTAVA, P., KANG, S., MILESI, C., ZHAO, M., JOSEPH, GLASSY, JOLLY, W. M., LOEHMAN, R., BOWKER, C. F., KIMBALL, J. S., NEMANI, R. R. & RUNNING, S. W. (2003) MOD17 User's Guide: GPP and NPP (MOD17A2/A3) Products *NASA MODIS Land Algorithm.*

HICKE, J. A., ASNER, G. P., RANDERSON, J. T., TUCKER, C., LOS, S., BIRDSEY, R., JENKINS, J. C. & FIELD, C. (2002) Trends in North American net primary productivity derived from satellite observations, 1982-1998. *Global Biogeochemical Cycles,* 16**,** 2-1.

JACOVIDES, C. P., TYMVIOS, F. S., ASIMAKOPOULOS, D. N., THEOFILOU, K. M. & PASHIARDES, S. (2003) Global photosynthetically active radiation and its relationship with global solar radiation in the Eastern Mediterranean basin. *Theoretical and Applied Climatology,* 74**,** 227-233.

KANIA, S. & GIACOMELLI, G. (2005) *Solar radiation availability for plant growth in Arizona controlled environment agriculture systems.*

KNMI (2003-2004) Daggegevens van het weer in Nederland. KNMI.

KNORR, W. & HEIMANN, M. (1995) Impact of drought stress and other factors on seasonal land biosphere CO2 exchange studied through an atmospheric tracer transport model. *Tellus, Series B,* 47 B**,** 471-489.

LAFONT, S., KERGOAT, L., DEDIEU, G., CHEVILLARD, A., KARSTENS, U. & KOLLE, O. (2002) Spatial and temporal variability of land CO2 fluxes estimated with remote sensing and analysis data over western Eurasia. *Tellus, Series B: Chemical and Physical Meteorology,* 54**,** 820-833.

LANDSBERG, J. J. & WARING, R. H. (1997) A generalised model of forest productivity using simplified concepts of radiation-use efficiency, carbon balance and partitioning. *Forest Ecology and Management,* 95**,** 209-228.

MILNER, K. S., RUNNING, S. W. & COBLE, D. W. (1996) A biophysical soil-site model for estimating potential productivity of forested landscapes. *Canadian Journal of Forest Research,* 26**,** 1174-1186.

MYNENI, R. B., HALL, F. G., SELLERS, P. J. & MARSHAK, A. L. (1995) Interpretation of spectral vegetation indexes. *IEEE Transactions on Geoscience and Remote Sensing,* 33**,** 481-486.

NEMANI, R. R., KEELING, C. D., HASHIMOTO, H., JOLLY, W. M., PIPER, S. C., TUCKER, C. J., MYNENI, R. B. & RUNNING, S. W. (2003) Climate-driven increases in global terrestrial net primary production from 1982 to 1999. *Science,* 300**,** 1560-1563.

NEMRY, B., FRANC?OIS, L., GE?RARD, J. C., BONDEAU, A. & HEIMANN, M. (1999) Comparing global models of terrestrial net primary productivity (NPP): Analysis of the seasonal atmospheric CO2 signal. *Global Change Biology,* 5**,** 65-76.

PAN, Y., BIRDSEY, R., HOM, J., MCCULLOUGH, K. & CLARK, K. (2006) Improved estimates of net primary productivity from modis satellite data at regional and local scales. *Ecological Applications,* 16**,** 125-132.

PINKER, R. T., LASZLO, I., WHITLOCK, C. H., AND & CHARLOCK, T. P. (1995) Radiative flux opens new window on climate research. *EOS Trans. AGU,* 76(15), 145.

POTTER, C. S., RANDERSON, J. T., FIELD, C. B., MATSON, P. A., VITOUSEK, P. M., MOONEY, H. A. & KLOOSTER, S. A. (1993) Terrestrial ecosystem production: A production model based on global satellite and surface data. . *Global Biogeochemical Cycles,* 7**,** 811-841.

PRINCE, S. D. & GOWARD, S. N. (1995) Global primary production: a remote sensing approach. *Journal of Biogeography,* 22**,** 815-835.

RAHMAN, A. F., CORDOVA, V. D., GAMON, J. A., SCHMID, H. P. & SIMS, D. A. (2004) Potential of MODIS ocean bands for estimating CO2 flux from terrestrial vegetation: A novel approach. *Geophysical Research Letters,* 31.

RAHMAN, A. F., GAMON, J. A., FUENTES, D. A., ROBERTS, D. A. & PRENTISS, D. (2001) Modeling spatially distributed ecosystem flux of boreal forest using hyperspectral indices from AVIRIS imagery. *Journal of Geophysical Research D: Atmospheres,* 106**,** 33579-33591.

RUIMY, A., DEDIEU, G. & SAUGIER, B. (1996) TURC: A diagnostic model of continental gross primary productivity and net primary productivity. *Global Biogeochemical Cycles,* 10**,** 269-285.

RUIMY, A., KERGOAT, L. & BONDEAU, A. (1999) Comparing global models of terrestrial net primary productivity (NPP): Analysis of differences in light absorption and light-use efficiency. *Global Change Biology,* 5**,** 56-64.

RUNNING, S. W., NEMANI, R. R., HEINSCH, F. A., ZHAO, M., REEVES, M. & HASHIMOTO, H. (2004) A continuous satellite-derived measure of global terrestrial primary production. *BioScience,* 54**,** 547-560.

RUNNING, S. W., THORNTON P. E., NEMANI R. & GLASSY, J. M. (2000) Global terrestrial gross and net primary productivity from the Earth Observing System. *Methods in Ecosystem Science***,** 44–57.

SALA, O. E., BIONDINI, M. E. & LAUENROTH, W. K. (1988) Bias in estimates of primary production: an analytical solution. *Ecological Modelling,* 44**,** 43-55.

TAO, F., YOKOZAWA, M., ZHANG, Z., XU, Y. & HAYASHI, Y. (2005) Remote sensing of crop production in China by production efficiency models: Models comparisons, estimates and uncertainties. *Ecological Modelling,* 183**,** 385-396.

TEILLET, P. M., CHICHAGOV, A., FEDOSEJEVS, G., GAUTHIER, R. P., AINSLEY, G., MALOLEY, M., GUIMOND, M., NADEAU, C., WEHN, H., SHANKAIE, A., YANG, J., CHEUNG, M., SMITH, A., BOURGEOIS, G., DE JONG, R., TAO, V. C., LIANG, S. H. L., FREEMANTLE, J. & SALOPEK, M. (2005) Overview of an intelligent sensorweb for integrated earth sensing project. *Proceedings of the 26th Canadian Symposium on Remote Sensing.*

TURNER, D. P., RITTS, W. D., COHEN, W. B., GOWER, S. T., ZHAO, M., RUNNING, S. W., WOFSY, S. C., URBANSKI, S., DUNN, A. L. & MUNGER, J. W. (2003)

Scaling Gross Primary Production (GPP) over boreal and deciduous forest landscapes in support of MODIS GPP product validation. *Remote Sensing of Environment,* 88**,** 256-270.

TURNER, D. P., RITTS, W. D., COHEN, W. B., MAEIRSPERGER, T. K., GOWER, S. T., KIRSCHBAUM, A. A., RUNNING, S. W., ZHAO, M., WOFSY, S. C., DUNN, A. L., LAW, B. E., CAMPBELL, J. L., OECHEL, W. C., KWON, H. J., MEYERS, T. P., SMALL, E. E., KURC, S. A. & GAMON, J. A. (2005) Site-level evaluation of satellite-based global terrestrial gross primary production and net primary production monitoring. *Global Change Biology,* 11**,** 666-684.

WHITE, M. A., THORNTON, P. E., RUNNING, S. W. & NEMANI, R. R. (2000) Parameterization and Sensitivity Analysis of the BIOME-BGC Terrestrial Ecosystem Model: Net Primary Production Controls. *Earth Interactions,* 4**,** 1-85.

Appendix

Appendix 1. Daily GPP

```
# ----------------------------------------------------------------------------
# gpp_result.py
# Created on: do jan 24 2008 03:23:27
#   (generated by ArcGIS/ModelBuilder)
# ----------------------------------------------------------------------------

# Import system modules
import sys, string, os, arcgisscripting

# Create the Geoprocessor object
gp = arcgisscripting.create()

# Check out any necessary licenses
gp.CheckOutExtension("spatial")

# Load required toolboxes...
gp.AddToolbox("C:/Program Files/ArcGIS/ArcToolbox/Toolboxes/Spatial Analyst Tools.tbx")


# Local variables...
v23sep_lue_par = "E:\\chuma_thesis\\TOP_tendata\\Emax\\LUE_PAR\\23sep_lue_par"
reclass_lgn4 = "E:\\chuma_thesis\\TOP_tendata\\reclass_lgn4"
value0 = "E:\\chuma_thesis\\TOP_tendata\\sep_lgn4\\value0"
noveg = "E:\\chuma_thesis\\TOP_tendata\\sep_lgn4\\noveg"
Cell_factor = "10"
Aggregation_technique = "SUM"
value_27 = "E:\\chuma_thesis\\TOP_tendata\\sep_lgn4\\value_27"
oshrub = "E:\\chuma_thesis\\TOP_tendata\\sep_lgn4\\oshrub"
value_30 = "E:\\chuma_thesis\\TOP_tendata\\sep_lgn4\\value_30"
grass = "E:\\chuma_thesis\\TOP_tendata\\sep_lgn4\\grass"
value_42 = "E:\\chuma_thesis\\TOP_tendata\\sep_lgn4\\value_42"
mx_forest = "E:\\chuma_thesis\\TOP_tendata\\sep_lgn4\\mx_forest"
value_300 = "E:\\chuma_thesis\\TOP_tendata\\sep_lgn4\\value_300"
cropland = "E:\\chuma_thesis\\TOP_tendata\\sep_lgn4\\cropland"
value_53 = "E:\\chuma_thesis\\TOP_tendata\\sep_lgn4\\value_53"
dbf_forest = "E:\\chuma_thesis\\TOP_tendata\\sep_lgn4\\dbf_forest"
value_140 = "E:\\chuma_thesis\\TOP_tendata\\sep_lgn4\\value_140"
nherb_veg = "E:\\chuma_thesis\\TOP_tendata\\sep_lgn4\\nherb_veg"

#read input file
file = open("E:\\chuma_thesis\\conv_efftable\\LUETminVPD.txt", "r")
file.readline()

while 1:
    try:
        rd_line = file.readline()
        if not line:
            break
        line = string.split(rd_line, "\t")
        col1 = string.strip(line[0])
        col2 = string.strip(line[1])
        col3 = string.strip(line[2])
        col4 = string.strip(line[3])
        col5 = string.strip(line[4])
        col6 = string.strip(line[5])
        col7 = string.strip(line[6])
        col8 = string.strip(line[7])
        col9 = "E:\\chuma_refdata\\ref_data\\NDVI_GRID\\ndvi_grid\\" + string.strip(line[8])

        output_location = "E:\\chuma_thesis\\TOP_tendata\\Emax\\final_GPP\\LP" + col1

        # Process: Single Output Map Algebra...
        term1 = "(%s * %s)" % (grass, col3)
        term2 = "(%s * %s)" % (oshrub, col7)
        term3 = "(%s * %s)" % (dbf_forest, col6)
        term4 = "(%s * %s)" % (mx_forest, col5)
        term5 = "(%s * %s)" % (cropland, col4)
        term6 = "(%s * 0)" % (noveg)
        term7 = "(%s * %s)" % (nherb_veg, col8)

        expression = "(((( %s + %s + %s + %s + %s + %s + %s) * 0.01) * %s) * %s)" % (term1,
                            term2, term3, term4, term5, term6, term7, col2, col9)
```

48

```
        gp.SingleOutputMapAlgebra_sa(expression, output_location)

        print "finished %s ...." % (col1)

    except:
        print gp.GetMessage(1)
        print gp.GetMessage(2)
```

Appendix 2. Table of ε per land use type and PAR (LUETminVPD)

date	PAR	grass(ε)	Cropland(ε)	mx_forest(ε)	dbf_forest(ε)	Oshrub(ε)	nherb_veg(ε)	NDVI_names
20070114	3.6920	0.1424	1.4236	0.2418	0.3159	0.1527	0.6643	ndvi2_jan14
20070203	5.8450	0.0614	0.6144	0.1044	0.1363	0.0659	0.2867	ndvi2_feb3
20070215	7.4514	0.0989	0.9890	0.1680	0.2194	0.1061	0.4615	ndvi2_feb15
20070310	10.7438	0.0929	0.9291	0.1578	0.2061	0.0996	0.4336	ndvi2_mr10
20070312	12.4766	0.1124	1.1239	0.1909	0.2494	0.1205	0.5245	ndvi2_mr12
20070313	11.4025	0.0809	0.8092	0.1375	0.1795	0.0868	0.3776	ndvi2_mr13
20070314	8.2526	0.0554	0.5544	0.0942	0.1230	0.0595	0.2587	ndvi2_mr14
20070315	11.7738	0.0689	0.6893	0.1171	0.1529	0.0739	0.3217	ndvi2_mr15
20070325	11.6274	0.1903	1.9031	0.3233	0.4223	0.2041	0.8881	ndvi2_mr25
20070326	14.7067	0.1935	1.9428	0.3248	0.4243	0.2077	0.9032	ndvi2_mr26
20070327	14.6830	0.2065	2.0787	0.3437	0.4489	0.2218	0.9638	ndvi2_mr27
20070328	14.8554	0.0989	0.9890	0.1680	0.2194	0.1061	0.4615	ndvi2_mr28
20070331	14.1763	0.1903	1.9031	0.3233	0.4223	0.2041	0.8881	ndvi2_mr31
20070401	15.9074	0.1959	1.9776	0.3227	0.4215	0.2105	0.9140	ndvi2_apr1
20070402	15.2377	0.1415	1.4240	0.2354	0.3074	0.1519	0.6602	ndvi2_apr2
20070404	16.8613	0.0869	0.8691	0.1476	0.1928	0.0932	0.4056	ndvi2_apr4
20070405	14.7906	0.0614	0.6144	0.1044	0.1363	0.0659	0.2867	ndvi2_apr5
20070406	15.3489	0.0884	0.8841	0.1502	0.1962	0.0948	0.4126	ndvi2_apr6
20070408	16.5007	0.0809	0.8092	0.1375	0.1795	0.0868	0.3776	ndvi2_apr8
20070412	17.1367	0.1214	1.2138	0.2062	0.2693	0.1302	0.5664	ndvi2_apr12
20070413	14.4789	0.2087	2.0887	0.3534	0.4617	0.2238	0.9738	ndvi2_apr13
20070414	17.7552	0.1620	1.6559	0.2560	0.3343	0.1745	0.7558	ndvi2_apr14
20070415	18.9608	0.1598	1.6384	0.2504	0.3271	0.1723	0.7459	ndvi2_apr15
20070416	18.1210	0.1439	1.4386	0.2444	0.3192	0.1543	0.6713	ndvi2_apr16
20070419	19.3159	0.0674	0.6743	0.1145	0.1496	0.0723	0.3147	ndvi2_apr19
20070422	20.0757	0.0914	0.9141	0.1553	0.2028	0.0980	0.4266	ndvi2_apr22
20070423	15.3800	0.1338	1.3476	0.2222	0.2902	0.1437	0.6244	ndvi2_apr23
20070425	16.1951	0.2487	2.5340	0.3566	0.4500	0.2444	1.1606	ndvi2_apr25
20070426	18.7389	0.2158	2.1578	0.3665	0.4788	0.2314	1.0070	ndvi2_apr26
20070427	19.7335	0.1409	1.4431	0.2216	0.2894	0.1519	0.6577	ndvi2_apr27
20070428	20.0517	0.1757	1.7925	0.2794	0.3650	0.1891	0.8197	ndvi2_apr28
20070429	21.6613	0.2474	2.5153	0.3631	0.4582	0.2471	1.1545	ndvi2_apr29
20070430	22.6959	0.1763	1.8001	0.2796	0.3653	0.1898	0.8226	ndvi2_apr30
20070501	22.2086	0.1835	1.8701	0.2930	0.3827	0.1975	0.8562	ndvi2_may1
20070502	22.6327	0.1584	1.6261	0.2465	0.3220	0.1707	0.7390	ndvi2_may2
20070503	20.2873	0.1229	1.2288	0.2087	0.2726	0.1318	0.5734	ndvi2_may3
20070504	18.6822	0.1433	1.4421	0.2389	0.3120	0.1539	0.6689	ndvi2_may4
20070505	21.5709	0.1783	1.7832	0.3029	0.3957	0.1913	0.8322	ndvi2_may5
20070523	24.4934	0.1513	1.5135	0.2571	0.3358	0.1623	0.7063	ndvi2_may23
20070524	24.1137	0.1866	1.8701	0.3150	0.4115	0.2002	0.8710	ndvi2_may24
20070530	22.6570	0.1364	1.3636	0.2316	0.3026	0.1463	0.6364	ndvi2_may30
20070602	19.4688	0.1991	1.9992	0.3339	0.4361	0.2137	0.9291	ndvi2_jun2
20070608	20.3232	0.2838	2.8661	0.3850	0.4859	0.2559	1.3243	ndvi2_jun8
20070611	14.8424	0.3000	3.0000	0.4200	0.5300	0.2700	1.4000	ndvi2_jun11
20070619	25.2697	0.1940	1.9521	0.3234	0.4224	0.2083	0.9055	ndvi2_jun19
20070708	19.8631	0.2962	2.9624	0.4200	0.5300	0.2700	1.3825	ndvi2_july8
20070719	19.0632	0.2843	2.8513	0.4097	0.5170	0.2659	1.3269	ndvi2_july19
20070801	21.8457	0.2538	2.5376	0.4200	0.5300	0.2700	1.1842	ndvi2_aug1
20070804	22.7785	0.2890	2.9029	0.4042	0.5101	0.2637	1.3488	ndvi2_aug4
20070805	23.1430	0.2435	2.5333	0.2982	0.3763	0.2209	1.1364	ndvi2_aug5
20070811	20.2921	0.2860	2.8599	0.4200	0.5300	0.2700	1.3346	ndvi2_aug11

20070923	11.4774	0.2450	2.4497	0.4161	0.5300	0.2627	1.1432	ndvi2_sep23
20071006	11.6497	0.2289	2.2886	0.3888	0.5078	0.2455	1.0680	ndvi2_oct6
20071007	10.8031	0.1922	1.9224	0.3266	0.4266	0.2062	0.8971	ndvi2_oct7
20071013	8.8504	0.2201	2.2007	0.3738	0.4883	0.2360	1.0270	ndvi2_oct13
20071014	10.0492	0.1966	1.9664	0.3340	0.4363	0.2109	0.9176	ndvi2_oct14
20071015	8.1470	0.2201	2.2007	0.3738	0.4883	0.2360	1.0270	ndvi2_oct15
20071022	8.5345	0.1498	1.4976	0.2544	0.3323	0.1606	0.6989	ndvi2_oct22
20071115	5.0641	0.0663	0.6627	0.1126	0.1470	0.0711	0.3093	ndvi2_nov15
20071122	4.1005	0.1893	1.8931	0.3216	0.4201	0.2030	0.8835	ndvi2_nov22
20071216	3.2264	0.0692	0.6920	0.1175	0.1535	0.0742	0.3229	ndvi2_dec16

Appendix 3. January-September growth respiration(Rg)

```
# -----------------------------------------------------------------------------
# 1A_dailyemax_ORIGINAL.py
# Created on: di jan 15 2008 02:49:22
#   (generated by ArcGIS/ModelBuilder)
# -----------------------------------------------------------------------------

# Import system modules
import sys, string, os, arcgisscripting

# Create the Geoprocessor object
gp = arcgisscripting.create()

# Enable overwrite output
gp.OverWriteOutput = 1

# Check out any necessary licenses
gp.CheckOutExtension("spatial")

# Load required toolboxes...
gp.AddToolbox("C:/Program Files/ArcGIS/ArcToolbox/Toolboxes/Spatial Analyst Tools.tbx")

i = 110
while i <= 999:
    try:
        # Set local variables
        OutRaster = "E:/chuma_thesis/TOP_tendata/Emax/Rg_resp2007/R20070" + str(i)
        InExpression = "E:/chuma_thesis/TOP_tendata/Emax/final_GPP/lp20070" + str(i)
        InExpression += " * 0.25"
        Input_raster = "E:/chuma_thesis/TOP_tendata/Emax/final_GPP/lp20070" + str(i)

        print InExpression
        print "output location: " + OutRaster

        # Process: Single Output Map Algebra...
        gp.SingleOutputMapAlgebra_sa(InExpression, OutRaster, Input_raster)
        i += 1

        print "finished OutRaster"

    except:
        # If an error occurred while running a tool, then print the messages.
        print gp.GetMessages(1)
        print gp.GetMessages(2)
        i += 1
```

Appendix 4. October-December growth respiration(Rg)

```
# -----------------------------------------------------------------------------
# 1A_dailyemax_ORIGINAL.py
# Created on: di jan 15 2008 02:49:22
#   (generated by ArcGIS/ModelBuilder)
# -----------------------------------------------------------------------------

# Import system modules
import sys, string, os, arcgisscripting

# Create the Geoprocessor object
gp = arcgisscripting.create()

# Enable overwrite output
gp.OverWriteOutput = 1
```

50

```
# Check out any necessary licenses
gp.CheckOutExtension("spatial")

# Load required toolboxes...
gp.AddToolbox("C:/Program Files/ArcGIS/ArcToolbox/Toolboxes/Spatial Analyst Tools.tbx")

i = 1000
while i <= 1231:
    try:
        # Set local variables
        OutRaster = "E:/chuma_thesis/TOP_tendata/Emax/Rg_resp2007/R2007" + str(i)
        InExpression = "E:/chuma_thesis/TOP_tendata/Emax/final_GPP/lp2007" + str(i)
        InExpression += " * 0.25"
        Input_raster = "E:/chuma_thesis/TOP_tendata/Emax/final_GPP/lp2007" + str(i)

        print InExpression
        print "output location: " + OutRaster

        # Process: Single Output Map Algebra...
        gp.SingleOutputMapAlgebra_sa(InExpression, OutRaster, Input_raster)
        i += 1

        print "finished OutRaster"

    except:
        # If an error occurred while running a tool, then print the messages.
        print gp.GetMessages(1)
        print gp.GetMessages(2)
        i += 1
```

Appendix 5. January-September Autotrophic respiration(Ra)

```
# Import system modules
import sys, string, os, arcgisscripting

# Create the Geoprocessor object
gp = arcgisscripting.create()

# Check out any necessary licenses
gp.CheckOutExtension("spatial")

# Load required toolboxes...
gp.AddToolbox("C:/Program Files/ArcGIS/ArcToolbox/Toolboxes/Spatial Analyst Tools.tbx")
gp.AddToolbox("C:/Program Files/ArcGIS/ArcToolbox/Toolboxes/Data Management Tools.tbx")


i = 110
while i <= 999:
    try:
        # Set local variables
        InExpression = "E:/chuma_thesis/Biomass/Rm_GRID/20070" + str(i)
        InExpression += "_ra + E:/chuma_thesis/TOP_tendata/Emax/Rg_resp2007/lp20070" + str(i)
        InExpression += "g"
        OutRaster = "E:/chuma_thesis/TOP_tendata/Emax/RmRgnew/rmrg20070" + str(i)

        print InExpression
        print "output location: " + OutRaster

        # Process: MapAlgebraStatement
        gp.SingleOutputMapAlgebra_sa(InExpression, OutRaster)
        i += 1

        print "finished OutRaster"

    except:
        # If an error occurred while running a tool, then print the messages.
        print gp.GetMessages()
        i += 1
```

Appendix 6. October-December Autotrophic respiration(Ra)

```
# Import system modules
import sys, string, os, arcgisscripting
```

```
# Create the Geoprocessor object
gp = arcgisscripting.create()

# Check out any necessary licenses
gp.CheckOutExtension("spatial")

# Load required toolboxes...
gp.AddToolbox("C:/Program Files/ArcGIS/ArcToolbox/Toolboxes/Spatial Analyst Tools.tbx")
gp.AddToolbox("C:/Program Files/ArcGIS/ArcToolbox/Toolboxes/Data Management Tools.tbx")


i = 1000
while i <= 1231:
    try:
        # Set local variables
        InExpression = "E:/chuma_thesis/Biomass/Rm_GRID/2007" + str(i)
        InExpression += "_ra + E:/chuma_thesis/TOP_tendata/Emax/Rg_resp2007/lp2007" + str(i)
        InExpression += "g"
        OutRaster = "E:/chuma_thesis/TOP_tendata/Emax/RmRgnew/rmrg2007" + str(i)

        print InExpression
        print "output location: " + OutRaster

        # Process: MapAlgebraStatement
        gp.SingleOutputMapAlgebra_sa(InExpression, OutRaster)
        i += 1

        print "finished OutRaster"

    except:
        # If an error occurred while running a tool, then print the messages.
        print gp.GetMessages()
        i += 1
```

Appendix 7. January-September Daily NPP

```
# Import system modules
import sys, string, os, arcgisscripting

# Create the Geoprocessor object
gp = arcgisscripting.create()

# Check out any necessary licenses
gp.CheckOutExtension("spatial")

# Load required toolboxes...
gp.AddToolbox("C:/Program Files/ArcGIS/ArcToolbox/Toolboxes/Spatial Analyst Tools.tbx")
gp.AddToolbox("C:/Program Files/ArcGIS/ArcToolbox/Toolboxes/Data Management Tools.tbx")


i = 110
while i <= 999:
    try:
        # Set local variables
        InExpression = "E:/chuma_thesis/TOP_tendata/Emax/final_GPP/lp20070" + str(i)
        InExpression += " - E:/chuma_thesis/TOP_tendata/Emax/RmRgnew/rmrg20070" + str(i)
        OutRaster = "E:/chuma_thesis/TOP_tendata/Emax/NPPdaily/npp20070" + str(i)

        print InExpression
        print "output location: " + OutRaster

        # Process: MapAlgebraStatement
        gp.SingleOutputMapAlgebra_sa(InExpression, OutRaster)
        i += 1

        print "finished OutRaster"

    except:
        # If an error occurred while running a tool, then print the messages.
        print gp.GetMessages()
        i += 1
```

Appendix 8. October-December Daily NPP

```
# Import system modules
import sys, string, os, arcgisscripting

# Create the Geoprocessor object
gp = arcgisscripting.create()

# Check out any necessary licenses
gp.CheckOutExtension("spatial")

# Load required toolboxes...
gp.AddToolbox("C:/Program Files/ArcGIS/ArcToolbox/Toolboxes/Spatial Analyst Tools.tbx")
gp.AddToolbox("C:/Program Files/ArcGIS/ArcToolbox/Toolboxes/Data Management Tools.tbx")


i = 1000
while i <= 1231:
     try:
          # Set local variables
          InExpression = "E:/chuma_thesis/TOP_tendata/Emax/final_GPP/lp2007" + str(i)
          InExpression += " - E:/chuma_thesis/TOP_tendata/Emax/RmRgnew/rmrg2007" + str(i)
          OutRaster = "E:/chuma_thesis/TOP_tendata/Emax/NPPdaily/npp2007" + str(i)

          print InExpression
          print "output location: " + OutRaster

          # Process: MapAlgebraStatement
          gp.SingleOutputMapAlgebra_sa(InExpression, OutRaster)
          i += 1

          print "finished OutRaster"

     except:
          # If an error occurred while running a tool, then print the messages.
          print gp.GetMessages()
          i += 1
```

Appendix 9. January-September Daily GPP upscaling (1000m)

```
# -------------------------------------------------------------------------
# GPPupscaling.py
# Created on: ma feb 11 2008 09:30:03
#   (generated by ArcGIS/ModelBuilder)
# -------------------------------------------------------------------------

# Import system modules
import sys, string, os, arcgisscripting

# Create the Geoprocessor object
gp = arcgisscripting.create()

#Enable overwrite output
gp.OverWriteOutput = 1

# Check out any necessary licenses
gp.CheckOutExtension("spatial")

# Load required toolboxes...
gp.AddToolbox("C:/Program Files/ArcGIS/ArcToolbox/Toolboxes/Spatial Analyst Tools.tbx")


i = 110
while i <= 999:
     try:
          # Local variables...
          OutRaster = "E:\\chuma_thesis\\TOP_tendata\\Emax\\GPPmean1000m\\lp20070" + str(i)
          InExpression = "E:\\chuma_thesis\\TOP_tendata\\Emax\\final_GPP\\lp20070" + str(i)
          Cell_factor = "4"
          Aggregation_technique = "MEAN"

          print InExpression
          print "output location: " + OutRaster

          # Process: Aggregate...
          gp.Aggregate_sa(InExpression, OutRaster, Cell_factor, Aggregation_technique, "EXPAND",
"DATA")
          i += 1
```

53

```
            print "finished OutRaster"

        except:
            # If an error occurred while running a tool, then print the messages.
            print gp.GetMessages(2)
            i += 1
```

Appendix 10. October-December Daily GPP upscaling (1000m)

```
# ---------------------------------------------------------------------------
# GPPupscaling.py
# Created on: ma feb 11 2008 09:30:03
#   (generated by ArcGIS/ModelBuilder)
# ---------------------------------------------------------------------------

# Import system modules
import sys, string, os, arcgisscripting

# Create the Geoprocessor object
gp = arcgisscripting.create()

#Enable overwrite output
gp.OverWriteOutput = 1

# Check out any necessary licenses
gp.CheckOutExtension("spatial")

# Load required toolboxes...
gp.AddToolbox("C:/Program Files/ArcGIS/ArcToolbox/Toolboxes/Spatial Analyst Tools.tbx")


i = 1000
while i <= 1231:
    try:
        # Local variables...
        OutRaster = "E:\\chuma_thesis\\TOP_tendata\\Emax\\GPPmean1000m\\lp2007" + str(i)
        InExpression = "E:\\chuma_thesis\\TOP_tendata\\Emax\\final_GPP\\lp2007" + str(i)
        Cell_factor = "4"
        Aggregation_technique = "MEAN"

        print InExpression
        print "output location: " + OutRaster

        # Process: Aggregate...
        gp.Aggregate_sa(InExpression, OutRaster, Cell_factor, Aggregation_technique, "EXPAND",
        "DATA")
        i += 1

        print "finished OutRaster"

    except:
        # If an error occurred while running a tool, then print the messages.
        print gp.GetMessages(2)
        i += 1
```

Appendix 11. January-September Daily NPP upscaling

```
# ---------------------------------------------------------------------------
# NPPupscaling.py
# Created on: ma feb 11 2008 09:30:03
#   (generated by ArcGIS/ModelBuilder)
# ---------------------------------------------------------------------------

# Import system modules
import sys, string, os, arcgisscripting

# Create the Geoprocessor object
gp = arcgisscripting.create()

#Enable overwrite output
gp.OverWriteOutput = 1

# Check out any necessary licenses
gp.CheckOutExtension("spatial")

# Load required toolboxes...
gp.AddToolbox("C:/Program Files/ArcGIS/ArcToolbox/Toolboxes/Spatial Analyst Tools.tbx")
```

```
i = 110
while i <= 999:
    try:
        # Local variables...
        OutRaster = "E:\\chuma_thesis\\TOP_tendata\\Emax\\NPPdaily1000m\\lp20070" + str(i)
        InExpression = "E:\\chuma_thesis\\TOP_tendata\\Emax\\NPPdaily\\npp20070" + str(i)
        Cell_factor = "4"
        Aggregation_technique = "MEAN"

        print InExpression
        print "output location: " + OutRaster

        # Process: Aggregate...
        gp.Aggregate_sa(InExpression, OutRaster, Cell_factor, Aggregation_technique, "EXPAND",
"DATA")
        i += 1

        print "finished OutRaster"

    except:
        # If an error occurred while running a tool, then print the messages.
        print gp.GetMessages(2)
        i += 1
```

Appendix 12. October-December Daily NPP upscaling

```
# ----------------------------------------------------------------------------
# NPPupscaling.py
# Created on: ma feb 11 2008 09:30:03
#   (generated by ArcGIS/ModelBuilder)
# ----------------------------------------------------------------------------

# Import system modules
import sys, string, os, arcgisscripting

# Create the Geoprocessor object
gp = arcgisscripting.create()

#Enable overwrite output
gp.OverWriteOutput = 1

# Check out any necessary licenses
gp.CheckOutExtension("spatial")

# Load required toolboxes...
gp.AddToolbox("C:/Program Files/ArcGIS/ArcToolbox/Toolboxes/Spatial Analyst Tools.tbx")


i = 1000
while i <= 1231:
    try:
        # Local variables...
        OutRaster = "E:\\chuma_thesis\\TOP_tendata\\Emax\\NPPdaily1000m\\lp2007" + str(i)
        InExpression = "E:\\chuma_thesis\\TOP_tendata\\Emax\\NPPdaily\\npp2007" + str(i)
        Cell_factor = "4"
        Aggregation_technique = "MEAN"

        print InExpression
        print "output location: " + OutRaster

        # Process: Aggregate...
        gp.Aggregate_sa(InExpression, OutRaster, Cell_factor, Aggregation_technique, "EXPAND",
"DATA")
        i += 1

        print "finished OutRaster"

    except:
        # If an error occurred while running a tool, then print the messages.
        print gp.GetMessages(2)
        i += 1
```

Appendix 13. MOD17A2 Unit Conversion (gC m-2)

```python
# ----------------------------------------------------------------------------
# MOD17A2.py
# Created on: do feb 14 2008 05:55:12
#   (generated by ArcGIS/ModelBuilder)
# ----------------------------------------------------------------------------

# Import system modules
import sys, string, os, arcgisscripting

# Create the Geoprocessor object
gp = arcgisscripting.create()

# Check out any necessary licenses
gp.CheckOutExtension("spatial")

# Load required toolboxes...
gp.AddToolbox("C:/Program Files/ArcGIS/ArcToolbox/Toolboxes/Spatial Analyst Tools.tbx")

i = 100
while i <= 999:
    try:
        # Local variables...
        OutRaster = "E:\\chuma_thesis\\TOP_tendata\\Emax\\MOD17A2_final\\c20070" + str(i)
        expression = "E:\\chuma_thesis\\TOP_tendata\\Emax\\MOD17A2_Rename1\\c20070" + str(i)
        expression += " * 0.1"
        In_raster = "E:\\chuma_thesis\\TOP_tendata\\Emax\\MOD17A2_Rename1\\c20070" + str(i)

        print Map_Algebra_expression
        print "output location: " + OutRaster

       # Process: Single Output Map Algebra...
        gp.SingleOutputMapAlgebra_sa(expression, OutRaster, In_raster)
        i += 1

        print "finished OutRaster"

    except:
        # If an error occurred while running a tool, then print the messages.
        print gp.GetMessages(2)
        i += 1


        print "finished OutRaster"

    except:
        # If an error occurred while running a tool, then print the messages.
        print gp.GetMessages(2)
        i += 1
```